

AperTO - Archivio Istituzionale Open Access dell'Università di Torino

Physicochemical properties and sorption capacities of sawdust-based biochars and commercial activated carbons towards ethoxylated alkylphenols and their phenolic metabolites in effluent wastewater from a textile district

This is the author's manuscript

Original Citation:

Availability:

This version is available <http://hdl.handle.net/2318/1739662> since 2020-05-22T14:05:06Z

Published version:

DOI:10.1016/j.scitotenv.2019.135217

Terms of use:

Open Access

Anyone can freely access the full text of works made available as "Open Access". Works made available under a Creative Commons license can be used according to the terms and conditions of said license. Use of all other works requires consent of the right holder (author or publisher) if not exempted from copyright protection by the applicable law.

(Article begins on next page)

Physicochemical properties and sorption capacities of sawdust-based biochars and commercial activated carbons towards ethoxylated alkylphenols and their phenolic metabolites in effluent wastewater from a textile district

Massimo Del Bubba^{a*}, Beatrice Anichini^b, Zaineb Bakari^{a,c}, Maria Concetta Bruzzoniti^d, Roberto Camisa^e, Claudia Caprini^a, Leonardo Checchini^a, Donatella Fibbi^e, Ayoub El Ghadraoui^a, Francesca Liguori^f, Serena Orlandini^a

^a Department of Chemistry “Ugo Schiff”, University of Florence, Via della Lastruccia 3 – 50019 Sesto Fiorentino, Florence, Italy

^b Publiacqua S.p.A., Via Villamagna 90/c – 50126 Florence, Italy

^c National Engineering School of Sfax, Route de la Soukra km 4 - 3038 Sfax, Tunisia

^d Department of Chemistry, University of Turin, Via Pietro Giuria 5 – 10125 Turin, Italy

^e GIDA S.p.A., Via di Baciacavallo 36, 59100 Prato, Italy

^f Institute for the Chemistry of Organometallic Compounds, National Research Council (ICCOM-CNR), Via Madonna del Piano 10 – 50019 Sesto Fiorentino, Florence, Italy

* Corresponding author: Massimo Del Bubba, Department of Chemistry, University of Florence, Via della Lastruccia 3, 50019 Sesto Fiorentino (Florence, Italy). Phone number: +39-055-4573326. E-mail: delbubba@unifi.it

1 **Abstract.** Three biochars were produced using sawdust from waste biomass, via a simple pyrolysis
2 thermal conversion at 450, 650, and 850 °C (BC450, BC650, and BC850), without any activation
3 process. These materials, together with vegetal and mineral commercial activated carbons (VAC and
4 MAC), were characterized for their elemental composition, Brunauer–Emmett–Teller surface area, t-
5 plot microporosity and Barrett-Joyner-Halenda mesoporosity. Moreover, iodine, phenol and
6 methylene blue porosity indexes were measured. The materials were also evaluated for their pH of
7 the point of zero charge, as well as near-surface chemical composition and surface functionality by
8 means of X-ray photoelectron and Fourier-transform infrared spectroscopy. Ash content, water-
9 extractable metals and polycyclic aromatic hydrocarbons (PAHs) were also determined. BC650
10 showed a much higher surface area ($319 \text{ m}^2 \text{ g}^{-1}$) compared to BC450 ($102 \text{ m}^2 \text{ g}^{-1}$), as well as an
11 increase in aromatization and the residual presence of functional polar groups. BC850 exhibited a
12 loss of polar and aromatic groups, with the dominance of graphitic carbon and the highest value of
13 surface area ($419 \text{ m}^2 \text{ g}^{-1}$). Biochars comply with the EN 12915-1/2009 limits for metal and PAH
14 release in water treatment. Biochars and MAC were tested using Langmuir and Freundlich isotherms
15 for the sorption in real effluent wastewater of a mixture of 14 branched ethoxylated 4-t-octyl and 4-
16 nonylphenols, as well as 4-t-octyl and 4-nonylphenol, the latter representing persistent, endocrine
17 disrupting contaminants, widespread in the effluents from wastewater treatment plants and listed as
18 priority/priority hazardous substances in the Directive 2013/39/EU. Biochars showed a lower
19 sorption efficiency compared to MAC. The best performance was found for BC650 towards the
20 alkylphenols (9-13 times less efficient than the MAC). Considering the lower market price of biochar
21 compared to MAC (estimated as at least 16 times less expensive by a small market survey), the former
22 can be considered more competitive than the latter.

23 **Keywords**

24 Porosimetry analyses; XPS; FTIR; Heavy-metal release; PAH release; Priority substances

25 **1. Introduction**

26 The quality of surface water (SW), as well as that of wastewater treated for reuse, is increasingly
27 compromised by the presence of organic micropollutants of both domestic and industrial origin.
28 Within this latter category, ethoxylated alkylphenols (AP_nEOs) with an alkyl chain length of eight
29 (OP_nEOs) or nine (NP_nEOs) carbon atoms must be taken into consideration due to their widespread
30 use and diffusion in the environment. These compounds are used mainly in the textile industry as
31 non-ionic surfactants, as well as antioxidants in a number of industrial applications (OSPAR
32 Commission, 2009). Even though AP_nEOs themselves are not carcinogenic, teratogenic or mutagenic,
33 it should be noted that toxicity, estrogenic activity, persistence and a tendency to bio-accumulate have
34 been highlighted for their alkylphenolic metabolites (APs) (Chiu et al., 2010; Ying, 2006). By means
35 of the Directive 2003/53/EC (European Parliament the Council, 2003), the European Community has
36 prohibited the use of nonylphenols (NPs) and NP_nEOs at concentrations higher than 0.1% in product
37 formulations. Furthermore, 4-t-octylphenols (4-t-OPs) and branched 4-NPs were listed as priority and
38 priority hazardous substances, and environmental quality standards of 0.1 µg/L and 0.3 µg/L,
39 respectively, have been established in the European regulations for inland SW (European Parliament
40 and Commission, 2013). However, the use of AP_nEOs with an alkyl chain length differing from nine
41 carbon atoms (e.g. OP_nEOs) is not restricted. Moreover, it must be underlined that no constraints are
42 in force in many non-European countries (e.g. China, Thailand), which are important exporters to
43 Europe of semi-finished textile products and fabric pre-treated with formulations containing 4-
44 NP_nEOs. Accordingly, the presence of AP_nEOs and their metabolites in effluents from wastewater
45 treatment plants (WWTPs) and fresh water in Europe has recently been highlighted by various authors
46 (Asimakopoulos et al., 2012; Loos et al., 2009; Månsson et al., 2008; Vega-Morales et al., 2010),
47 especially in the textile districts (Ciofi et al., 2014; Ciofi et al., 2016). Hence, these compounds are
48 still of environmental concern in European water-ecosystems and their efficient removal by WWTPs
49 should be considered a hot topic. In this regard, biological treatments are not effective for providing

50 “zero emissions” of organic micropollutants and an important role can be played by adsorption
51 techniques based on well-established materials (i.e. activated carbons) or innovative adsorbents (e.g.
52 polymer-derived silicon carbide foams and aerogels or mesoporous silica “as such” or properly
53 functionalized) (Bruzzoniti et al., 2016; Bruzzoniti et al., 2018; Prasanta et al., 2016; Rivoira et al.,
54 2016).

55 In recent years, increasing attention has also been paid to the use of biochars, as low-cost adsorbent
56 materials obtained from pyro-gasification of waste vegetal biomass and/or biosolids (Ahmad et al.,
57 2014; Peiris et al., 2017; Tan et al., 2015). As these waste materials are readily available, at a low or
58 even no cost, they could be conveniently recycled for preparing biochars to be used in the removal of
59 organic micropollutants in wastewaters. In fact, if the biomass used for biochar production is a waste
60 product, its disposal involves a cost, whereas its reuse is in line with the modern approach to resource
61 management and the circular economy, thereby ensuring great savings. In addition, if the feedstock
62 is an invasive species, conversion into biochar could improve its management and also protect the
63 environment (Dong et al., 2013). Finally, it should be noted that lower temperatures are usually
64 required to produce biochar compared to activated carbon (Zheng et al., 2010), with significant
65 energy savings. Hence, the conversion of biomass into biochar as a sorbent for wastewater/water
66 treatment seems to be a “win–win” solution for both improving waste management and protecting
67 the environment.

68 Biochar is a porous material, rich in aromatic groups, containing both a crystalline fraction similar to
69 graphene and an amorphous fraction, in which organic carbon is linked to groups with different
70 polarity (Ahmad et al., 2014; Tan et al., 2015). However, different materials, characterized by a vast
71 physical and chemical heterogeneity (Bucheli et al., 2014; Zhao et al., 2013), with a considerable
72 variability in their physicochemical properties, are obtained in relation to the feedstock, thermo-
73 chemical process and pre-treatment of biomass and/or post-treatment of biochar (Lofrano, 2012).
74 Indeed, biochar can be modified and/or engineered following different approaches (e.g. chemical and

75 physical activation, metal impregnation and functionalization), in order to enhance their adsorption
76 performance (Liu et al., 2015a; Tan et al., 2017) and/or widen the range of molecules that can be
77 efficiently removed (Sun et al., 2019). However, engineered biochars have their own limitations,
78 including the consumption and/or the release of chemicals or nanomaterials that are of environmental
79 concern, as well as the high cost of large-scale production (Lyu et al., 2018; Wan et al., 2019).

80 The study of biochar as a sorbent medium of organic compounds from water highlights the promising
81 sorption capabilities of these materials (Ahmad et al., 2014; Mandal et al., 2017; Peiris et al., 2017;
82 Tan et al., 2015; Zheng et al., 2019). Even though the published studies focused on a wide range of
83 model compounds of environmental concern, to the best of our knowledge, no studies have been
84 reported on the adsorption of AP_nEOs and APs from water by biochars. Furthermore, it should be
85 noted that sorption studies of organic micropollutants are usually performed on ultrapure water, also
86 modified for pH and/or ionic strength and/or organic matter content (Jung et al., 2013; Reguyal and
87 Sarmah, 2018; Zheng et al., 2019). However, background properties of solutions used for adsorption
88 studies strongly affect the results obtained (Xiang et al., 2019). Therefore, it would be advisable to
89 perform these studies using the aqueous matrixes intended to be treated with biochar as background
90 solutions (Li et al., 2019). Conversely, as far as we know, isotherm studies on sorption of organic
91 micropollutants have only been performed in real wastewater in one case (Shimabuku et al., 2016).

92 In addition, the published studies focus mostly on the adsorption of only one or a few molecules at a
93 time, thus only allowing a partial interpretation of the competitive effects on the adsorption
94 phenomena. It is also worth noting that in most cases no comparison has been made with the
95 adsorption capacity of standard activated carbons, with obvious limitations in the reliable evaluation
96 of the sorption performance of biochars.

97 Based on the aforementioned considerations, this research has focused on the investigation of the
98 sorption performance of biochars produced from sawdust at different temperatures towards a wide
99 range of AP_nEOs and APs (i.e. 16 molecules belonging to homologue series with very different

100 physicochemical properties) in effluent wastewater from a local WWTP operating in an industrial
101 textile district. Adsorption capacities of biochars were compared with those obtained with
102 commercial activated carbons, commonly used in WWTPs and drinking water facilities. Sorption
103 performance was discussed in relation to some physicochemical properties of the materials in order
104 to interpret the removal data obtained. Biochars were also evaluated for their release of heavy metals
105 and polycyclic aromatic hydrocarbons (PAHs), as requested for activated carbons to be used in water
106 and wastewater treatment.

107 **2. Materials and Methods**

108 Full details of the reagents, standards and materials used in this research, as well as preparation of
109 stock solutions of target analytes, are reported in paragraph S.1 of the Supplementary material, in
110 which CAS numbers, structure formulas and log K_{OW} values of the investigated AP_nEOs and APs are
111 also shown (**Table S1**).

112 *2.1 Effluent wastewater used in sorption studies*

113 Kinetic and isotherm sorption studies were performed in a real effluent wastewater obtained from the
114 Baciacavallo WWTP operating in the industrial textile district of Prato (Italy). The WWTP consisted
115 in a primary sedimentation, biological oxidation, secondary sedimentation, clariflocculation and final
116 ozonation treatment. The effluent wastewater was sampled in August 2018, during the summer
117 closure of the industrial textile district in order to minimize the concentration of target analytes in the
118 wastewater (Berardi et al., 2019). The characterization of the effluent wastewater for a number of
119 routinely analysed parameters, as well as target analytes, is shown in **Table S2** (paragraph S.2 of the
120 Supplementary material). The results presented in Table S2 for APs and AP_nEOs showed that the
121 WWTP effluent contained APs and AP_nEOs at concentrations much lower than the lowest spiked
122 level in the matrix.

123 2.2 *Biochars and activated carbons*

124 Three biochars (BC450, BC650 and BC850) were produced via pyrolysis of sawdust, in a muffle
125 furnace (Gefran 1001, Vittadini Strumentazione, Milano, Italy), at 450, 650 and 850°C, respectively,
126 with a contact time of 60 min. The following yield percentages (mean \pm standard deviation) were
127 registered in the 15 pyrolysis processes performed for each temperature: BC450 – 23 \pm 3; BC650 –
128 20.0 \pm 0.7; BC850 – 18.1 \pm 0.5. The temperature of 450°C was chosen since it represents a minimum
129 temperature value allowing the pyrolysis process to fully proceed on woody matrices. In fact, wood
130 contains large amounts of lignin, the complete decomposition of which only occurs at around 500°C
131 (Ok et al., 2018). The highest temperature limit was selected as intermediate between the maximum
132 values investigated in literature (i.e. 800-900°C) (Li et al., 2017), whereas the value of 650°C was
133 equally spaced between 450 and 850°C.

134 The muffle furnace was properly modified to allow the heating process in N₂-saturated conditions.
135 The sawdust was obtained from a local sawmill and consisted of a mixture of waste biomass from
136 broad-leaved and coniferous plants. The water content of sawdust and concentrations of selected toxic
137 heavy metals are reported in **Table S3** of the Supplementary material. Metal analysis was performed
138 by acidic-oxidant digestion (Doumett et al., 2011) followed by ICP-MS analysis, with the only
139 exception of Cr(VI) which was determined according to Bruzzoniti et al. (Bruzzoniti et al., 2017).
140 Full details of these analyses are reported in paragraph S.3 of the Supplementary material.

141 Virgin mineral activated carbon (MAC) was obtained from Arkema (Colombes, France). Virgin
142 vegetal activated carbon (VAC) was purchased from SICAV (Chieti, Italy).

143 All chars were pre-treated before being characterized and used in isotherm studies. More specifically,
144 the materials were sieved at 45 μ m and then repeatedly washed with Milli-Q water according to the
145 ASTM D-5919-96 method (American Society for Testing and Material, 1996).

146 2.3 *Char characterization*

147 2.3.1. *Elemental analysis*

148 The analyses of C, H, N and S were performed using a FlashEA® 1112 elemental analyser Thermo
149 Fisher Scientific (Waltham, MA) equipped with a thermal conductivity detector. The percentage
150 content of oxygen was estimated as the difference with those of the other elements and ash (Al-Wabel
151 et al., 2013). Moreover, the O/C and H/C ratios were calculated and plotted in a van Krevelen diagram
152 (**Figure S1** of the Supplementary material). Full details of the elemental analysis and related
153 calculations are reported in paragraph S.4.1 of the Supplementary material.

154 2.3.2. *Physisorption analyses*

155 Physisorption analysis of biochars, MAC and VAC was performed via nitrogen adsorption and
156 desorption experiments using a Porosity Analyser Micrometrics (Norcross, GA, USA) model ASAP
157 2020 (American Society for Testing and Materials, 2012; American Society for Testing and
158 Materials, 2017). More in detail, the total surface area and micropore surface area were determined
159 respectively by the Brunauer–Emmett–Teller (BET) method and by t-plot method, whereas mesopore
160 surface area and average pore width were measured by the Barrett-Joyner-Halenda (BJH) method
161 applied to desorption data. See paragraph S.4.2 and **Table S4** in the Supplementary material for full
162 experimental details and porosimetry results.

163 2.3.3. *Porosity indexes*

164 The analyses of the porosity indexes were performed following the official methods for activated
165 carbons and regarded the determination of iodine (American Society for Testing and Materials, 1994),
166 phenol (American Water Works Association, 1978) and methylene blue indexes (European Council
167 of Chemical Manufacturers' Federation, 1986). The results of these characterizations are illustrated
168 in **Table S5**, whereas the correlation between porosity indexes and porosimetry data are shown in
169 **Figure S2** (paragraph S.4.3 of the Supplementary material).

170 2.3.4. *pH of the point of zero charge*

171 The pH of the point of zero charge (pH_{pzc}) of biochars and MAC was determined using the pH drift
172 method, which is a simple and widely used procedure, adopted for the evaluation of surface charge
173 of both biochars (Chaukura et al., 2017) and activated carbons (Niasar et al., 2016). Full details of
174 the procedure and the plot of the results obtained (**Figure S3**) are reported in paragraph S.4.4 of the
175 Supplementary material.

176 2.3.5. *X-ray photoelectron spectroscopy analysis*

177 The chemical composition of the near surface sample portion was investigated by means of X-ray
178 Photoelectron Spectroscopy (XPS) as described in detail in paragraph S.4.5 of the Supplementary
179 material. Experimental XPS peak areas were normalized using proper sensitivity factors (Moulder et
180 al., 1992) in order to calculate the relative element percentages (see **Table S6**).

181 2.3.6. *Fourier-transform infrared analysis*

182 Fourier-transform infrared (FTIR) analyses were performed on a Shimadzu IRAffinity-1
183 Spectrometer equipped with a single-reflection diamond ATR crystal on ZnSe plate (MIRacle™
184 Single Reflection ATR, PIKE Technologies). Samples were dried beforehand in a muffle furnace at
185 120°C for 24 h.

186 2.3.7. *Ash content*

187 Ash content was determined according to the EN 12902:2004 Official Method (European Committee
188 for Standardization, 2004), which is adopted for the analysis of activated carbons.

189 2.3.8. *Water-extractable substances*

190 The following water extractable elements were determined: As, Cd, Cr, Hg, Ni, Pb, Sb, Se, Al, Ba,
191 B, Ca, Fe, Mg, Mn, K, Cu, Na, Va and Zn. Moreover, the 16 PAHs included in the EPA mixture (see
192 paragraph S.1 of the Supplementary material) were analysed.

193 The extraction of the aforementioned inorganic and organic species was performed according to the
194 EN 12902:2004 standard method (European Committee for Standardization, 2004), as described in
195 full in paragraph S.5 of the Supplementary material.

196 The analysis of the water-extractable metals was carried out by ICP-MS, based on to the USEPA SW-
197 846 test method 6020 B (USEPA, 2014). Full details of this analytical protocol are reported in
198 paragraph S.5.1 of the Supplementary material.

199 PAH were determined by SPE extraction and GC-MS analysis, as described in paragraph S.5.2 of the
200 Supplementary material. Figures of merit and apparent recovery of the method are shown in **Tables**
201 **S7-S9** and **Figure S4**.

202 *2.4 Performance evaluation of chars as adsorbent materials*

203 The evaluation of biochar and activated carbon adsorption performance towards AP_nEOs and APs
204 was carried out by kinetic and isotherm tests, performed in triplicate.

205 In line with the ASTM D-5919-96 (American Society for Testing and Material, 1996), suspensions
206 (1 g L⁻¹) of each adsorbent material were prepared, stirred for 24 h and used to make solutions of
207 biochars (10 mg L⁻¹) and MAC (1 mg L⁻¹) with proper AP_nEO and AP concentrations. These solutions
208 were used to perform kinetic and isotherm adsorption tests as fully specified in paragraph S.6 of the
209 Supplementary material. LC-MS/MS analysis of AP_nEOs and APs at the end of the tests was
210 performed following the identification criteria proposed by the Commission Decision 2002/657/EC
211 (The Commission of the European Communities, 2002), according to a method optimized specifically
212 for this study. Full details of LC-MS/MS method are provided in paragraph S.6 and **Tables S10-S12**
213 of the Supplementary material.

214 *2.4.1. Kinetic adsorption tests*

215 Kinetic adsorption tests of target compounds on biochars and MAC were performed using solutions
216 of APs (40 µg L⁻¹), TritonTMX-45 and IGEPAL® CO-520 technical mixtures (400 µg L⁻¹) in the

217 aforementioned real effluent wastewater. These experiments were carried out by maintaining the test
218 bottles in rotation at T=20°C with contact times of 1, 2, 4, 6, and 12 h.

219 2.4.2. Isotherm adsorption tests

220 Isotherm experiments were conducted using eleven different concentration levels of AP_nEO technical
221 mixtures (i.e. 0, 5, 10, 25, 50, 75, 100, 150, 200, 300, and 400 µg L⁻¹) and APs (i.e. 0, 0.5, 1.0, 2.5,
222 5.0, 7.5, 10, 15, 20, 30, and 40 µg L⁻¹) in the aforementioned real effluent wastewater, keeping the
223 concentration of the adsorbent materials constant. These experiments were carried out by maintaining
224 the test bottles in rotation for 4 h at T=20° C, in accordance with results of the kinetic tests.

225 Adsorption data were fitted by using both Langmuir and Freundlich equations. More specifically, the
226 following Langmuir adsorption-isotherm equation (Equation 1) was adopted:

$$227 \quad Q_e = \frac{Q_m \cdot k \cdot C_e}{1 + (k \cdot C_e)} \quad (1)$$

228 where C_e is the equilibrium adsorbate concentration (mg L⁻¹), Q_e the mass of adsorbate per mass unit
229 of adsorbent at equilibrium (mg g⁻¹), Q_m the maximum mass adsorbed at saturation conditions per
230 mass unit of adsorbent (mg g⁻¹) and k (L mg⁻¹) the empirical constant with units of inverse of
231 concentration C_e . The linear form of the above-mentioned equation is reported in Equation 2.

$$232 \quad \frac{C_e}{Q_e} = \frac{1}{Q_m \cdot k} + \frac{1}{Q_m} \cdot C_e \quad (2)$$

233 which represents a straight line with slope Q_m^{-1} and intercept $(Q_m k)^{-1}$ (Del Bubba et al., 2003).

234 Accordingly, linearized Langmuir adsorption-isotherm equation allows for estimating both the Q_m
235 and k , the latter representing the inverse of the equilibrium concentration of the adsorbate at half
236 saturation and thereby giving a measure of the affinity of the compound for the material.

237 The Freundlich isotherm model can be written as:

$$238 \quad \log Q_e = \log K_F + \frac{1}{n} \cdot \log C_e \quad (3)$$

239 where Q_e and C_e have the same aforementioned meaning, while K_F and n are the Freundlich constants
240 related to adsorption capacity and intensity, respectively (Sun et al., 2013).

241 2.5 *Data treatment and computational analysis*

242 The multiple comparison of the mean values of the sorption parameters was performed using the non-
243 parametric Games-Howell test (Minitab®17.1.0, Minitab Inc., State College, PA, USA), which
244 makes it possible to compare mean values and corresponding standard deviations without assuming
245 equal variances of the measured variables.

246 Molecular weight of target analytes was calculated after energy minimization by Chem3D version
247 12.0.2.1076 (PerkinElmer Informatics, Waltham, MA, USA).

248 **3. Results and discussion**

249 Based on log K_{ow} data (3.49-5.79) shown in **Table S1** of the Supplementary material, the target
250 molecules covered a quite wide range of hydrophobicity, making the study informative of the
251 adsorption properties of synthesized biochars for molecules characterized by low-to-medium polarity.

252 3.1 *Physicochemical characterizations of chars*

253 Sorbent materials to be used for water and wastewater treatment are commonly characterized for their
254 elemental composition, surface area and presence of functional groups both involved in the adsorption
255 capacities towards the organic micropollutants. In this study, CHNS elemental analysis, BET total
256 surface area, micropore and mesopore distribution, as well as pH_{pzc} , XPS and FTIR data on surface
257 functionalization were provided. Furthermore, in water treatment plants (WTPs) and WWTPs the
258 selection of activated carbons is performed via the determining of parameters related to sorption
259 efficiency, porosity indexes (i.e. iodine, phenol and methylene blue numbers) and ash content. The
260 porosity indexes, which are still used in research papers for comparing sorption properties of activated
261 carbons (Jian et al., 2018), were also evaluated and discussed in relation to the instrumental
262 porosimetry results.

263 3.1.1. *Elemental analysis*

264 Data concerning C, H, N, S, and O analysis are presented in **Table 1**. The results showed very small
265 percentages of nitrogen in all the investigated materials. Furthermore, sulphur was only found in
266 MAC, even though at very low percentages. As observed elsewhere, the abundance of these elements
267 in biochars depends mainly on the feedstock characteristics (Ahmad et al., 2014).

268 Pyrolysis temperature played a significant role in changing the biochar characteristics, as evaluated
269 by elemental analysis. The carbon content strongly increased with the rise in the pyrolysis
270 temperature and a corresponding loss of H, N, and O was recorded. More specifically, much higher
271 percentage variations were found from 450 °C to 650 °C for C and O, whereas for H the percentage
272 decrease was quite homogeneous among the three biochars. The increase in carbon content with a
273 rise in temperature is attributed to an enhanced carbonization degree of the material, which is related
274 to the increasing formation of well-organized graphitized layers (Ahmad et al., 2014). The decline in
275 H, N, and O can be ascribed to the defunctionalisation of the materials that involves a loss of polar
276 groups. Accordingly, as shown by the van Krevelen diagram (see **Fig. S1**), lower molar H/C and O/C
277 ratios are observed in biochars with a rise in the pyrolysis temperature. The diagram also highlights
278 that between the two activated carbons considered, MAC is the one most similar to the biochars
279 obtained in this study.

280 3.1.2. *Porosimetry results*

281 **Table 2** illustrates the results obtained for the porosimetry analyses (i.e. BET total surface area, t-
282 plot micropore surface area and BJH desorption cumulative mesopore surface area) of all the
283 investigated materials. In accordance with data in literature (Inyang and Dickenson, 2015), biochar
284 surface areas increased with a rise in the production temperature, from 102 to 419 m² g⁻¹. Hence, in
285 this study, the highest BET surface area measured for biochars was approximately half that
286 determined for commercial activated carbons used as comparators. To understand the overall
287 significance of BET data obtained here, it is also interesting to compare them with the values reported

288 in literature for the numerous biochars obtained from vegetal feedstocks, including woody sawdust.
289 However, in this regard, it should be noted that besides pyrolysis temperature and time, also the type
290 of vegetal feedstock strongly affects the surface area of biochars. For example, for the 8 feedstocks
291 from broad-leaved and/or coniferous species pyrolysed at temperatures above 600 °C for which BET
292 data are available in literature, an interval between 2 (fir sawdust pyrolysed at 600 °C) (Chen et al.,
293 2019) and 637 m² g⁻¹ (pine wood shaving pyrolysed at 700 °C) (Chen et al., 2016) was observed, with
294 an average of 278±189 m² g⁻¹ and a median of 347 m² g⁻¹ (Ahmad et al., 2014; Chen et al., 2016;
295 Chen et al., 2019; Ghani et al., 2013; Li et al., 2016; Tan et al., 2015; Wang et al., 2015). Therefore,
296 the BET surface areas of the sawdust-based biochars obtained in this study between 650 and 850 °C
297 (i.e. 319 and 419 m² g⁻¹) are fully comparable with those in literature.

298 The distribution of micropores (pore diameter <2 nm), mesopores (2–50 nm), and macropores (>50
299 nm) of a material is important in determining its adsorptive capacity (Li et al., 2016). In our materials,
300 microporosity was higher than mesoporosity irrespective of the pyrolysis temperature (**Table 2**).
301 Even though the microporosity-to-mesoporosity ratio and their trends with temperature depends on
302 various experimental conditions (e.g. the feedstock and the temperature), in biochars deriving from
303 coniferous and/or broad-leaved tree residues a prevalence of microporosity has been widely reported
304 (Shimabuku et al., 2016; Xiao and Pignatello, 2015; Zhu et al., 2018). Data from our study highlighted
305 a major increase in microporosity (i.e. a threefold augment) from 450 °C to 650 °C that was by far
306 the main factor responsible for the corresponding high increase in total surface area within this
307 temperature range. Conversely, the rise in the pyrolysis temperature from 650 °C to 850 °C led to a
308 much more limited increase in microporosity (approximately 17%), whereas the surface area of
309 mesopores was almost tripled. Interestingly, on the rather limited panorama of studies concerning the
310 micropore/mesopore distribution in biochars produced in a wide range of temperatures from woody
311 species, the temperature trends observed in this study for microporosity and mesoporosity were

312 similar to those reported elsewhere for biochars deriving from maple and pine wood waste (Xiao and
313 Pignatello, 2015; Zhu et al., 2018).

314 The iodine, phenol and methylene blue indexes are commonly determined in activated carbons in
315 order to evaluate their quality as sorbents, due to the relation between these indexes and pore
316 distribution (Zhang et al., 2007). More in detail, iodine and phenol indexes should be related to the
317 presence of micropores and therefore be informative of the effectiveness in removing small-size
318 organic water pollutants. On the other hand, methylene blue index should be linked to the abundance
319 of mesopores and thus be a useful indicator of adsorption capacities for medium-large sized organic
320 pollutants. Higher values of methylene blue and especially iodine index, as well as corresponding
321 enhanced adsorptions of phenol, were observed with a rise in the pyrolysis temperature (**Table S5**).
322 It is worth noting that the three indexes showed a good linear correlation ($R^2 \geq 0.976$) with temperature
323 (graphs not shown).

324 The behaviour of the iodine index is in line with other studies (e.g. for rice husk derived biochar)
325 (Jian et al., 2018) The modest increase of the methylene blue index with a rise in temperature was
326 also in accordance with data reported elsewhere (Irfan et al., 2016; Jian et al., 2018). Very good linear
327 correlations ($R^2=0.928-0.996$) were observed between surface area and adsorption indexes (see **Fig.**
328 **S2A-C**). Moreover, high correlations were found between iodine/phenol indexes and micropore
329 surface area ($R^2=0.932-0.962$, **Fig. S2D-E**), as well as between the methylene blue index and
330 mesopore surface area ($R^2=0.890$, **Fig. S2F**), thus confirming the physical significance of these
331 indexes in describing structural properties of sorbents. However, these correlations were only found
332 to be strong when considering biochars produced in the same experimental conditions (e.g. same
333 feedstock), with the only exception of the pyrolysis temperature. In fact, the inclusion of VAC and
334 MAC, as well as other biochars produced in our laboratory from other feedstocks strongly lowered
335 the correlations (data not shown).

336 As regards VAC and MAC, porosimetry data highlighted a much higher total surface area and
337 mesoporosity in the latter (**Table 2**). In this regard, literature data showed that AP_nEO adsorption by
338 ACs is mainly related to the mesopore abundance (Liu et al., 2006) as well as surface area. Hence,
339 considering also the results of the elemental analysis on VAC and MAC, the latter was selected as
340 the reference material for the following investigations.

341 3.1.3. *Point of zero charge*

342 The results of the pH measurements at the point of zero charge of biochars and MAC (see **Fig. S3**)
343 were included in quite a narrow range (7.15-7.78). Since the mean value of pH of the effluent
344 wastewater used in this study was 7.46 (see **Table S2**), it can be assumed that no significant charge
345 was present at the surface of the investigated materials. It should also be noted that AP_nEOs do not
346 have any dissociable acid-base groups in water. APs, which have the phenol group characterized by
347 a pK_a value of about ten, are neutral at the pH of the effluent wastewater. Accordingly, sorption
348 mechanisms based on ionic interactions are not present in the experimental conditions adopted here.

349 3.1.4. *XPS analysis*

350 The results of the XPS analyses for the elements carbon and oxygen in BC450, BC650, BC850 and
351 MAC are reported in **Figure 1**. The assignment of the various XPS binding energy peaks can be
352 performed according to practical guidelines for the interpretation of XPS spectra (Thermo Fisher
353 Scientific, 2019a; Thermo Fisher Scientific, 2019b). The analysis of nitrogen did not highlight the
354 presence of any significant signal (data not shown), in accordance with the very low nitrogen
355 percentages determined via elemental analysis (**Table 1**). The biochar produced at 450°C showed a
356 very broad carbon peak (**Fig. 1A**), covering a larger range of binding energy compared to what was
357 observed in the three other materials (**Fig. 1B-D**). More specifically, binding energies typically
358 associated with C-O-C (about 286 eV), C=O (about 287 eV) and O-C=O (about 288.5 eV) moieties
359 were largely represented in the carbon peak of BC450, whilst much less chemical diversity was
360 observed in BC650, BC850 and MAC, in agreement with their higher production temperature. Similar

361 considerations can be deduced from XPS spectra of oxygen, which showed a much broader peak for
362 BC450 (**Fig. 1E**), compared to the others (**Fig. 1F-H**), in any case covering the values of binding
363 energies compatible with C=O (about 531.5 eV) and C-O (about 533.5 eV) groups. Quantitative data
364 obtained from the normalized peak areas of XPS spectra (see **Table S6**) showed an increase in the
365 carbon percentage and a corresponding decrease of oxygen with the rise in temperature from 450 °C
366 to 650 °C, while no significant variations were observed above this temperature. Interestingly,
367 percentages of carbon and oxygen in the surface of biochars were very similar to the values
368 determined by elemental analysis in the bulk materials (**Table 1**), suggesting a good degree of
369 homogeneity.

370 3.1.5. FTIR analysis

371 **Figure 2** illustrates the results of the FTIR analyses for BC450, BC650, BC850 and MAC, obtained
372 in the wave number region between 1,800 and 600 cm^{-1} , which is the most sensitive to structural
373 changes occurring in biochars as a function of the production temperature range investigated (Fu et
374 al., 2012; Wang et al., 2015). The FTIR spectra of biochars reflected changes in their surface
375 functional groups in relation to the different production temperatures. The spectroscopic assignments
376 of the various FTIR absorption bands can be performed according to practical guidelines in literature
377 for the interpretation of FTIR spectra (Coates, 2006). The FTIR spectrum of BC450 highlighted a
378 band at about 1600 cm^{-1} , which can be attributed to the stretching of a C=O group conjugated with a
379 C=C or an aromatic ring, as well as the aromatic ring itself. Stretching of aromatic C–O groups,
380 related to the presence of the phenolic and/or ether moieties, is the cause of the broad absorption band
381 centred at about 1205 cm^{-1} (Coates, 2006). This band was almost completely maintained in the BC650
382 spectrum, which also showed a shift to lower wavenumbers of the band at about 1600 cm^{-1} , probably
383 due to the partial loss of polar functional groups and the simultaneous increase in aromatization. This
384 latter modification was also evidenced by the increase of the absorptions in the wavenumber range
385 700-900 cm^{-1} , which are related to the aromatic C-H out-of-plane bending. The further increase of

386 the pyrolysis temperature to 850°C conversely resulted in the loss of polar and aromatic groups up to
387 the dominance of graphitic carbon (Liu et al., 2015b), thus obtaining a FTIR spectra very similar to
388 the one determined for MAC.

389 Overall, the FTIR findings are in agreement with the results of XPS discussed above, showing how
390 BC650 possesses intermediate characteristics compared to the other materials tested, in terms of
391 presence of polar group and degree of aromatization.

392 3.1.6. Ash

393 In biochars, ash percentages were in the narrow range of 1.74-2.30%, with the lowest value achieved
394 at 650°C (**Table S5**). These values were comparable with that determined in VAC ($2.13\pm 0.04\%$),
395 whereas a much higher ash content was found in MAC ($8.02\pm 0.03\%$). Literature data generally
396 showed an increasing ash content with the rise in pyrolysis temperature (Ahmad et al., 2014; Kearns
397 et al., 2014; Zhao et al., 2013). However, the extent of this increase is strongly influenced by the
398 feedstock used for biochar production, due to the mineral quantity and organic matter combustion
399 residues. Furthermore, ash content is obviously affected by the washing procedure of chars. As a
400 result, a very wide range of values are reported in literature, even considering only vegetal feedstocks
401 (0.3-58%) (Ahmad et al., 2014). Hence, ash percentages found in this study were among the lowest
402 determined in previously published papers.

403 3.2 Water-extractable metals and PAHs

404 Concentrations of water-extractable metals and PAHs of biochars and MAC are shown in **Table 3**
405 and **Table 4**, in comparison with values included in EN 12915-1/2009 (European Committee for
406 Standardization, 2009), which provides limits for pollutant release from products used for the
407 treatment of water intended for human consumption.

408 3.2.1. *Metals*

409 All biochars complied with the EN 12915-1/2009 limits for metal release (European Committee for
410 Standardization, 2009). In most cases, the data of **Table 3** evidenced values below the method
411 quantification limits (MQLs) or comparable with blank contributions. The main exceptions were Al
412 in BC850 and MAC, Mn and Ba in all biochars, as well as As in MAC, the last found at $11 \mu\text{g L}^{-1}$,
413 which is slightly higher than the European Regulation limit. Ba and Mn were actually the only two
414 metals exhibiting much higher leachable concentrations in biochars than MAC. However, these
415 metals are not included in the EN 12915-1/2009.

416 No clear effect was observed for the release of heavy metals as a function of pyrolysis temperature,
417 even though for Fe and particularly Al, a much higher leaching was determined in BC850 compared
418 to BC450 (**Table 3**). The release of this latter metal was by far the greatest found in the investigated
419 elements, suggesting a high native abundance in the feedstock. In this regard, it should be noted that
420 Al was found elsewhere to be the most abundant metal in sawdust (Sarkar et al., 2014).

421 The much higher Al release by BC850 and MAC could be related to the high production temperature,
422 which generally promotes the increase in surface area and porosity of the material, as well as the
423 decrease in the surface oxygenated functional groups (Harvey et al., 2011; McBeath et al., 2011). In
424 this regard, according to literature, surface area and porous structure of biochar seem to affect heavy
425 metal adsorption less than oxygen-containing functional groups, which may exhibit strong
426 interactions such as electrostatic attraction, ion-exchange and surface complexation (Tan et al., 2015).

427 As observed elsewhere, Na, K, Mg and Ca should be monitored in biochar leachate as possible causes
428 of salinity increase in treated water, since these elements are naturally found at mg g^{-1} levels in
429 biochars (Brewer et al., 2017). Concentrations observed in this study were comparable, or lower than
430 those previously found in aqueous leachate of biochars produced from *Atriplex* species (Brewer et
431 al., 2017). Moreover, Na, K, Mg and Ca concentrations found in biochar leachate were similar to

432 those found for MAC, which are used for the treatment of drinking water without any significant
433 contribution to their salinity.

434 3.2.2. PAHs

435 As shown in **Table S9** of the Supplementary material, the overall MQLs in extraction water were
436 found in the range of 0.13 – 0.9 ng L⁻¹. These limits were fully suitable for PAH determination in the
437 extraction water, according to EN 12915-1/2009 (European Committee for Standardization, 2009),
438 which requires leachable concentrations ≤ 20 ng L⁻¹ for the sum of fluoranthene,
439 benzo(b)fluoranthene, benzo(k)fluoranthene, benzo(a)pyrene, indeno(1,2,3-cd)pyrene and
440 benzo(a)pyrene (**Table 4**). All sorbents showed leachable PAH concentrations from sub-ng L⁻¹ to
441 low- ng L⁻¹ levels in accordance with the EN 12915-1/2009 limits. It must be noted that for all the
442 investigated PAHs, leachable concentrations decreased as the production temperature of the biochars
443 increased, in line with recently published results on 16 USEPA PAHs content in biochars produced
444 at different temperatures (De la Rosa et al., 2019). Furthermore, phenanthrene was found to be the
445 most abundant water-extractable PAH in all the biochars, in agreement with data reported elsewhere
446 regarding biochars from wood biomass (Keiluweit et al., 2012).

447 3.3 Adsorption efficiency

448 The evaluation of AP_nEO and AP sorption by biochars and MAC (used as reference material) was
449 performed by kinetic and isotherm analyses.

450 3.3.1. Kinetic test

451 **Figure 3** illustrates the adsorption kinetics obtained with the four materials investigated for APs and
452 AP₈EOs, which respectively represent the most hydrophobic and hydrophilic compounds considered
453 in this study, whereas the complete removal dataset is shown in **Tables S13-S16** (paragraph S.6.1 of
454 the Supplementary material). Data shown in **Fig. 3** clearly showed how the highest increase in
455 sorption of APs and AP₈EOs was highlighted by passing from one to two hours of contact time. Two

456 additional hours of contact time did not provide any further increase in the removal, except for 4-t-
457 OP₈EO with BC650 (**Table S14**) and 4-t-OP₅EO for BC850 (**Table S15**), whereas contact times of 6
458 and 12 h did not offer any increase in removal. These results showed a fast adsorption kinetic for all
459 carbons, in agreement with the fact that biochars were sieved at 45 µm and then purified by washing
460 before being used in adsorption studies. According to the results of the adsorption kinetic study, a
461 contact time of 4 h was selected for the isotherm test.

462 3.3.2. Isotherm analysis

463 Modelling the removal of organic micropollutants by adsorption isotherms is a widely accepted
464 approach in the scientific community for evaluating and comparing the adsorption performance of
465 sorbent materials, including carbons (Chen, 2015). Both Langmuir and Freundlich equations have
466 been largely adopted for the investigation of sorption properties of biochars towards organic
467 micropollutants in aqueous solution (Tan et al., 2015). The two equations were a good fit with the
468 experimental data obtained, with determination coefficients (R^2) always higher than 0.92. However,
469 in all cases the Langmuir model provided two different trends of C_e/Q_e values as a function of C_e ,
470 with comparable R^2 values. More specifically, much higher slopes of the regression lines and
471 corresponding lower Q_m ($Q_{m,1}$) values were determined for the initial concentration ranges of 5-100
472 µg L⁻¹ (for AP_nEOs) and 0.5-10 µg L⁻¹ (for APs), compared to the higher ones ($Q_{m,2}$) obtained at 100-
473 400 µg L⁻¹ (for AP_nEOs) and 10-40 µg L⁻¹ (for APs). Analogously, much lower values of the empirical
474 constant k were calculated based on the higher concentration range compared to the lower one. **Table**
475 **S17** illustrates the two Q_m data sets calculated by the linearized Langmuir equation, while the two
476 series of k values are shown in **Table S18** (paragraph S.6.2 of the Supplementary material). The
477 presence of two trends in the Langmuir isotherms has been demonstrated previously as generally
478 valid for any experimental sorption isotherm such those obtained in this study, in which the mass
479 adsorbed is a concave function of the equilibrium concentration that asymptotically approaches a

480 maximum value (Sposito, 1982). Based on these considerations, it is evident that no physical
481 significance should be attributed to the presence of the two trends of C_e/Q_e vs. C_e .
482 The linearized Freundlich isotherm model fitted the experimental data by a single trend of $\log Q_e$ vs.
483 $\log C_e$. **Table 5** shows the K_F values determined by the linearized Freundlich equation, while the n
484 data are reported in **Table S19** (paragraph S.6.2 of the Supplementary material).
485 Interestingly, the adsorption capacity parameters calculated by the two equations (i.e. $Q_{m,1}$ and $Q_{m,2}$;
486 K_F) within each homologue series and material were quite well correlated ($0.67 \leq R^2 \leq 0.98$; $P < 0.05$),
487 highlighting similar trends of the adsorption capacity measured through the two parameters, as a
488 function of the number of ethoxylate units.
489 Regardless of the physical meaning attributable to the Langmuir parameters Q_m and k , or their
490 corresponding K_F and n of the Freundlich equation, it is nonetheless interesting to make some
491 comments common to both isotherm equations. In this regard, according to literature, biochar can act
492 as a sorbent of organic molecules through various mechanisms including the formation of hydrogen
493 bonds, as well as electrostatic, π - π and hydrophobic interactions (Tan et al., 2015). The adsorption
494 capacities of biochars, estimated by Q_m or K_F values, were much lower than those found for MAC,
495 irrespective of the compound considered, revealing the lower sorption performances of the former
496 materials. Within each char, the sorption of the nonyl derivative (more hydrophobic) was higher than
497 that of the corresponding octyl (less hydrophobic); furthermore, biochars and especially MAC
498 showed the highest adsorption capacity for 4-NP, which represent the most hydrophobic compound
499 among those investigated. These findings highlighted the presence of important hydrophobic
500 interactions regulating the sorption of the investigated molecules on biochars and MAC. Therefore,
501 in order to evaluate a possible relation between sorption capacity of the four materials investigated
502 and the polarity of the target analytes, it is possible to plot the values of Q_m or K_F as a function of \log
503 K_{OW} of 4-t-OP_nEOs and 4-t-OP. Conversely, for 4-NP_nEOs contained in the IGEPAL®CO-520
504 technical mixture, it was not possible to draw a similar plot, since $\log K_{OW}$ values were not available

505 for some branched nonyl oligomers (see **Table S1**). The trends observed for Q_m or K_F as a function
506 of $\log K_{OW}$ of octyl derivatives were nearly overlapping and therefore only the plots of K_F values
507 (which represent a single dataset) are reported. Accordingly, **Figure 4** illustrates the profile of K_F
508 values as a function of $\log K_{OW}$ of 4-t-OP and 4-t-OP_nEOs. For all materials, the linear trend only
509 partially fitted the K_F versus $\log K_{OW}$ data. More in detail, MAC exhibited linearity in the widest
510 range of ethoxylation, from eight to four ethoxylate units, whilst compounds with a lower
511 ethoxylation degree and 4-t-OP showed an erratic trend. On the whole, these findings are in
512 accordance with the results of XPS and FTIR that evidenced the absence of aromaticity and polar
513 functional groups for MAC, thus making hydrophobic interactions predominant. For biochars, the
514 deviation from linearity started from 4-t-OP₃EO (BC450 and BC850) and 4-t-OP₄EO (BC650). These
515 deviations may depend on the multiple interactions governing the sorption of organic compounds on
516 chars. Moreover, it is important to underline that the isothermal sorption experiments were conducted
517 using a WWTP effluent which contains organic compounds differing from those investigated that are
518 able to compete with the adsorption sites of the materials, thus making the data interpretation even
519 more complex. Among the deviations from linearity observed in biochars for the K_F versus $\log K_{OW}$
520 trend, it must also be observed that for BC450, and especially BC650 and BC850 (**Fig. 4A-C**), the
521 sorption capacities of 4-t-OP₈EO and 4-t-OP₇EO were approximately the same. This latter finding is
522 probably related to the exclusion of the oligomers with 7-8 ethoxylate units from the pores of the
523 biochars, which are for the most part in the micropore range. In fact, the molecular width of these
524 oligomers (approximately from 3.25 to 3.50 nm) falls within the dimensional range of the mesopores.
525 In this regard, it is interesting to note that in MAC, this exclusion phenomenon did not occur since
526 the material is predominantly mesoporous (see **Table 2**).

527 Considering the effect of the pyrolysis temperature on sorption estimated by the K_F values, the data
528 reported in **Table 5** showed that in almost all cases BC450 exhibited the lowest sorption capacity, in
529 agreement with its lower surface area and micro/mesoporosity development. For 4-t-OP and 4-NP –

530 the smallest analytes within the group of molecules investigated (molecular width about 0.8-1.0 nm)
531 – a sharp improvement of the sorption capacity was found from 450 °C to 650 °C, followed by a
532 similar sharp decrease from 650 °C to 850 °C. This result is in full agreement with XPS and FTIR
533 data which, as a whole, highlighted for BC650 the highest degree of aromatization (very important
534 for sorption by π - π interactions) and the residual presence of polar functional groups that can
535 contribute to sorption via the hydrogen bond and/or other polar interactions. More similar adsorption
536 capacities were found for the other compounds, even though BC850 behaved slightly better for 4-t-
537 OP_nEOs with n=2-6, while BC650 was more effective for the corresponding nonyl derivatives.

538 3.3.3. *Evaluation of sorption performances of biochars in comparison with MAC*

539 Freundlich isotherm is empirical, whereas the Langmuir equation is based on very different model
540 assumptions from the experimental conditions related to the adsorption of solvated molecules,
541 especially in a real effluent wastewater such as the one used in this study. It is therefore evident that
542 the model parameters of Langmuir (Q_m and k) and Freundlich (K_F and n) equations cannot be
543 interpreted as fully significant values of adsorption capacity and intensity. However, these data can
544 be compared with those obtained in the same experimental conditions using a reference sorbent
545 material (i.e. MAC), and thereby obtaining more meaningful information for evaluating the removal
546 performance of biochars. To this end, a relative adsorption index (AI%) can be calculated for each
547 target compound as the percentage ratio of the adsorption capacities of biochars and MAC, using the
548 K_F values for their evaluation (see **Figure 5**). AI% values were in the ranges of 3.5-6.0, 3.5-11.2 and
549 3.4-7.3, for BC450, BC650 and BC850, respectively. Overall, far higher AI% values were obtained
550 with BC650 for 4-t-OP (11.2%) and 4-NP (7.9%), which are listed in the Directive 2013/39/EU
551 (European Parliament and Commission, 2013) as priority and priority hazardous substances and must
552 therefore be considered of major environmental importance. Even though these sorption
553 performances are 9-13 times lower than that of MAC, it should be stressed that they were obtained
554 by a simple pyrolytic thermal conversion of a recycled biomass at a relatively low temperature

555 (650°C), without any activation process. BC650 was also the best performing material for the sorption
556 of 4-NP_nEOs. However, the performance differences among materials were much more similar than
557 those observed for APs, and approximately 17-25 times worse than MAC. Conversely, for 4-t-
558 OP_nEOs with n=2-5, the best removal performance was obtained with BC850, which provided a
559 relative sorption performance approximately 14 times lower than MAC. BC850 was also the best
560 performing material for t-OP₆EO, with a removal performance about 16 times lower compared to
561 MAC and more similar to BC450, and especially BC650 (**Fig. 5**). Still lower removal performances
562 were found for 4-t-OP₈EO and above all for 4-t-OP₇EO, the latter showing the same sorption by the
563 three biochars (see **Table 5**).

564 3.3.4. *Cost comparison between biochar and activated carbon*

565 A market survey that involved the water potabilization companies of Tuscany (Italy) has shown that
566 they obtain activated carbon at a wholesale price (i.e. 2.1-2.6 €/kg). The biochar produced in Italy is
567 not currently used as water filtering material. However, the production of biochar from waste vegetal
568 biomass similar to those in this study used as feedstock of the pyrolysis process, is now starting up in
569 Italy in the soil amendment market. According to the information provided by RM Impianti S.r.l.
570 (Arezzo, Italy), currently the largest biochar producer in Tuscany, this material is currently
571 commercialized in the agricultural sector at a price of approximately 0.15 €/kg, which could of course
572 be lowered in case of supplies comparable to those of activated carbons in WTPs. Consequently, a
573 price of biochar at least 16 times lower than that of activated carbon can be considered plausible,
574 making biochar competitive with the marketed activated carbon, at least for the removal of APs,
575 which, as mentioned above, have shown a sorption performance 9-13 times lower than that of MAC.

576 **4. Conclusions**

577 For the first time, this research has provided information on sorption by biochars in real effluent
578 wastewater of a mixture of AP_nEOs and APs which are very widespread micropollutants of
579 environmental concern in wastewater and surface water.

580 All biochars produced in this study using mixed coniferous and broad-leaved waste biomass, within
581 a pyrolysis temperature range of 450-850 °C, complied with the EN 12915-1/2009 limits for metal
582 and PAH leaching in water and provided a negligible contribution to the release of salts in the treated
583 water.

584 The sorption of AP_nEOs and APs by BC450, BC650, BC850, and MAC showed a lower performance
585 of biochars in comparison with activated carbon. The sorption by biochars was governed by multiple
586 interaction mechanisms, which were more or less significant depending on the pyrolysis temperature
587 and the resulting characteristics of the materials. In particular, BC650 showed the presence of surface
588 aromatic domains and polar functionalities, together with a quite high surface area (319 m² g⁻¹),
589 achieving the best sorption performance towards 4-t-OP and 4-NP (i.e. 9-13 times lower than those
590 determined with MAC), which are the target analytes of the greatest environmental concern among
591 those investigated. However, considering the cheaper market price of biochar compared to activated
592 carbons (at least 16 times less expensive), the former can be considered commercially competitive
593 with the latter and hence worth being further investigated for future applications in water and
594 wastewater treatment. It should also be emphasized that the production and use of biochar from waste
595 biomass is in line with the modern approach to resource management and the circular economy.

596 **Acknowledgements**

597 The authors are grateful to the Fondazione Cassa di Risparmio di Firenze (Italy) and Regione Toscana
598 (POR FSE 2014-2020 Asse A – Occupazione, Grant Number 172781 – Project GREENCLEAN) for
599 their financial support. They also wish to thank Susan Mary Cadby for her linguistic revision of the
600 paper.

601 **References**

- 602 Ahmad M, Rajapaksha AU, Lim JE, Zhang M, Bolan N, Mohan D, et al. Biochar as a sorbent for
603 contaminant management in soil and water: A review. *Chemosphere* 2014; 99: 19-33.
- 604 Al-Wabel MI, Al-Omran A, El-Naggar AH, Nadeem M, Usman AR. Pyrolysis temperature induced
605 changes in characteristics and chemical composition of biochar produced from conocarpus
606 wastes. *Bioresource technology* 2013; 131: 374-379.
- 607 American Society for Testing and Material. Standard Practice for Determination of Adsorptive
608 Capacity of Activated Carbon by a Micro-Isotherm Technique for Adsorbates at ppb
609 Concentrations (ASTM D5919-96). ASTM International, West Conshohocken, PA, 1996.
- 610 American Society for Testing and Materials. Standard Test Method for Determination of Iodine
611 Number of Activated Carbon (ASTM-D4607-94). West Conshohocken, PA: ASTM
612 International, 1994.
- 613 American Society for Testing and Materials. Standard Test Method for Carbon Black—Total and
614 External Surface Area by Nitrogen Adsorption (ASTM-D6556-10). West Conshohocken, PA:
615 ASTM International, 2012.
- 616 American Society for Testing and Materials. Standard Practice for Calculation of Pore Size
617 Distributions of Catalysts and Catalyst Carriers from Nitrogen Desorption Isotherms (ASTM-
618 D4641-17). West Conshohocken, PA: ASTM International, 2017.
- 619 American Water Works Association. B600-78, Standard for Powdered Activated Carbon. AWWA,
620 1978.
- 621 Asimakopoulos AG, Thomaidis NS, Koupparis MA. Recent trends in biomonitoring of bisphenol A,
622 4-t-octylphenol, and 4-nonylphenol. *Toxicology letters* 2012; 210: 141-154.
- 623 Berardi C, Fibbi D, Coppini E, Renai L, Caprini C, Scordo CVA, et al. Removal efficiency and mass
624 balance of polycyclic aromatic hydrocarbons, phthalates, ethoxylated alkylphenols and
625 alkylphenols in a mixed textile-domestic wastewater treatment plant. *Science of The Total
626 Environment* 2019; 674: 36-48.

- 627 Brewer CE, Sarpong KA, Amiri A, Smith MB, Idowu OJ. Effects of Pyrolysis Conditions on
628 Leaching of Salts from Halophyte Biochars. 2017 ASABE Annual International Meeting.
629 ASABE, St. Joseph, MI, 2017, pp. 1.
- 630 Bruzzoniti M, De Carlo R, Rivoira L, Del Bubba M, Pavani M, Riatti M, et al. Adsorption of
631 bentazone herbicide onto mesoporous silica: application to environmental water purification.
632 Environmental Science and Pollution Research 2016; 23: 5399-5409.
- 633 Bruzzoniti MC, Abollino O, Pazzi M, Rivoira L, Giacomino A, Vincenti M. Chromium, nickel, and
634 cobalt in cosmetic matrices: an integrated bioanalytical characterization through total content,
635 bioaccessibility, and Cr(III)/Cr(VI) speciation. Analytical and Bioanalytical Chemistry 2017;
636 409: 6831-6841.
- 637 Bruzzoniti MC, Appendini M, Rivoira L, Onida B, Del Bubba M, Jana P, et al. Polymer-derived
638 ceramic aerogels as sorbent materials for the removal of organic dyes from aqueous solutions.
639 Journal of the American Ceramic Society 2018; 101: 821-830.
- 640 Bucheli TD, Bachmann HJ, Blum F, Bürge D, Giger R, Hilber I, et al. On the heterogeneity of biochar
641 and consequences for its representative sampling. Journal of Analytical and Applied Pyrolysis
642 2014; 107: 25-30.
- 643 Chaukura N, Murimba EC, Gwenzi W. Sorptive removal of methylene blue from simulated
644 wastewater using biochars derived from pulp and paper sludge. Environmental Technology
645 & Innovation 2017; 8: 132-140.
- 646 Chen D, Chen X, Sun J, Zheng Z, Fu K. Pyrolysis polygeneration of pine nut shell: quality of
647 pyrolysis products and study on the preparation of activated carbon from biochar. Bioresource
648 technology 2016; 216: 629-636.
- 649 Chen W, Wei R, Yang L, Yang Y, Li G, Ni J. Characteristics of wood-derived biochars produced at
650 different temperatures before and after deashing: Their different potential advantages in
651 environmental applications. Science of the Total Environment 2019; 651: 2762-2771.
- 652 Chen X. Modeling of experimental adsorption isotherm data. Information 2015; 6: 14-22.

- 653 Chiu TY, Paterakis N, Cartmell E, Scrimshaw MD, Lester JN. A critical review of the formation of
654 mono- and dicarboxylated metabolic intermediates of alkylphenol polyethoxylates during
655 wastewater treatment and their environmental significance. *Critical Reviews in*
656 *Environmental Science and Technology* 2010; 40: 199-238.
- 657 Ciofi L, Ancillotti C, Chiuminatto U, Fibbi D, Checchini L, Orlandini S, et al. Liquid
658 chromatographic–tandem mass spectrometric method for the simultaneous determination of
659 alkylphenols polyethoxylates, alkylphenoxy carboxylates and alkylphenols in wastewater and
660 surface-water. *Journal of Chromatography A* 2014; 1362: 75-88.
- 661 Ciofi L, Ancillotti C, Chiuminatto U, Fibbi D, Pasquini B, Bruzzoniti MC, et al. Fully automated on-
662 line solid phase extraction coupled to liquid chromatography–tandem mass spectrometry for
663 the simultaneous analysis of alkylphenol polyethoxylates and their carboxylic and phenolic
664 metabolites in wastewater samples. *Analytical and bioanalytical chemistry* 2016; 408: 3331-
665 3347.
- 666 Coates J. Interpretation of infrared spectra, a practical approach. *Encyclopedia of analytical*
667 *chemistry: applications, theory and instrumentation* 2006.
- 668 De la Rosa JM, Sánchez-Martín ÁM, Campos P, Miller AZ. Effect of pyrolysis conditions on the
669 total contents of polycyclic aromatic hydrocarbons in biochars produced from organic
670 residues: Assessment of their hazard potential. *Science of The Total Environment* 2019; 667:
671 578-585.
- 672 Del Bubba M, Arias CA, Brix H. Phosphorus adsorption maximum of sands for use as media in
673 subsurface flow constructed reed beds as measured by the Langmuir isotherm. *Water*
674 *Research* 2003; 37: 3390-3400.
- 675 Dong D, Yang M, Wang C, Wang H, Li Y, Luo J, et al. Responses of methane emissions and rice
676 yield to applications of biochar and straw in a paddy field. *Journal of soils and sediments*
677 2013; 13: 1450-1460.
- 678 Doumett S, Fibbi D, Azzarello E, Mancuso S, Mugnai S, Petruzzelli G, et al. Influence of the
679 application renewal of glutamate and tartrate on Cd, Cu, Pb and Zn distribution between

680 contaminated soil and paulownia tomentosa in a pilot-scale assisted phytoremediation study.
681 International Journal of Phytoremediation 2011; 13: 1-17.

682 European Committee for Standardization. EN 12902:2004, Products Used for Treatment of Water
683 Intended for Human Consumption - Inorganic Supporting and Filtering Materials - Methods
684 of Test, 2004.

685 European Committee for Standardization. EN 12915:2009, Products used for the treatment of water
686 intended for human consumption - Granular Activated Carbon, 2009.

687 European Council of Chemical Manufacturers' Federation. Test Method for Activated Carbon, 1986.

688 European Parliament and Commission. Directive 2013/39/EU of the European Parliament and of the
689 Council of 12 August 2013 amending Directives 2000/60/EC and 2008/105/EC as regards
690 priority substances in the field of water policy. Off. J. Eur. Union 2013; 226: 1-17.

691 European Parliament the Council. Directive 2003/53/EC of the European Parliament and of the
692 Council of 18 June 2003 Amending for the 26th time Council Directive 76/769/EEC Relating
693 to Restrictions on the Marketing and Use of Certain Dangerous Substances and Preparations
694 (nonylphenol, nonylphenol ethoxylate and cement), 2003.

695 Fu P, Hu S, Xiang J, Sun L, Su S, An S. Study on the gas evolution and char structural change during
696 pyrolysis of cotton stalk. Journal of Analytical and Applied Pyrolysis 2012; 97: 130-136.

697 Ghani WAWAK, Mohd A, da Silva G, Bachmann RT, Taufiq-Yap YH, Rashid U, et al. Biochar
698 production from waste rubber-wood-sawdust and its potential use in C sequestration:
699 Chemical and physical characterization. Industrial Crops and Products 2013; 44: 18-24.

700 Harvey OR, Herbert BE, Rhue RD, Kuo L-J. Metal interactions at the biochar-water interface:
701 energetics and structure-sorption relationships elucidated by flow adsorption
702 microcalorimetry. Environmental Science & Technology 2011; 45: 5550-5556.

703 Inyang M, Dickenson E. The potential role of biochar in the removal of organic and microbial
704 contaminants from potable and reuse water: A review. Chemosphere 2015; 134: 232-240.

- 705 Irfan M, Chen Q, Yue Y, Pang R, Lin Q, Zhao X, et al. Co-production of biochar, bio-oil and syngas
706 from halophyte grass (*Achnatherum splendens* L.) under three different pyrolysis
707 temperatures. *Bioresource Technology* 2016; 211: 457-463.
- 708 Jian X, Zhuang X, Li B, Xu X, Wei Z, Song Y, et al. Comparison of characterization and adsorption
709 of biochars produced from hydrothermal carbonization and pyrolysis. *Environmental
710 Technology & Innovation* 2018; 10: 27-35.
- 711 Jung C, Park J, Lim KH, Park S, Heo J, Her N, et al. Adsorption of selected endocrine disrupting
712 compounds and pharmaceuticals on activated biochars. *Journal of hazardous materials* 2013;
713 263: 702-710.
- 714 Kearns JP, Wellborn LS, Summers RS, Knappe DRU. 2,4-D adsorption to biochars: Effect of
715 preparation conditions on equilibrium adsorption capacity and comparison with commercial
716 activated carbon literature data. *Water Research* 2014; 62: 20-28.
- 717 Keiluweit M, Kleber M, Sparrow MA, Simoneit BRT, Prahlg FG. Solvent-Extractable Polycyclic
718 Aromatic Hydrocarbons in Biochar: Influence of Pyrolysis Temperature and Feedstock.
719 *Environmental Science & Technology* 2012; 46: 9333-9341.
- 720 Li H, Dong X, da Silva EB, de Oliveira LM, Chen Y, Ma LQ. Mechanisms of metal sorption by
721 biochars: biochar characteristics and modifications. *Chemosphere* 2017; 178: 466-478.
- 722 Li L, Zou D, Xiao Z, Zeng X, Zhang L, Jiang L, et al. Biochar as a sorbent for emerging contaminants
723 enables improvements in waste management and sustainable resource use. *Journal of Cleaner
724 Production* 2019; 210: 1324-1342.
- 725 Li S, Lü J, Zhang T, Cao Y, Li J. Relationship between biochars' porosity and adsorption of three
726 neutral herbicides from water. *Water Science and Technology* 2016; 75: 482-489.
- 727 Liu G, Zheng S, Yin D, Xu Z, Fan J, Jiang F. Adsorption of aqueous alkylphenol ethoxylate
728 surfactants by mesoporous carbon CMK-3. *Journal of Colloid and Interface Science* 2006;
729 302: 47-53.

- 730 Liu W-J, Jiang H, Yu H-Q. Development of biochar-based functional materials: toward a sustainable
731 platform carbon material. *Chemical Reviews* 2015a; 115: 12251-12285.
- 732 Liu Y, He Z, Uchimiya M. Comparison of biochar formation from various agricultural by-products
733 using FTIR spectroscopy. *Modern Applied Science* 2015b; 9: 246.
- 734 Lofrano G. Green technologies for wastewater treatment: energy recovery and emerging compounds
735 removal: Springer Science & Business Media, 2012.
- 736 Loos R, Gawlik BM, Locoro G, Rimaviciute E, Contini S, Bidoglio G. EU-wide survey of polar
737 organic persistent pollutants in European river waters. *Environmental Pollution* 2009; 157:
738 561-568.
- 739 Lyu H, Gao B, He F, Zimmerman AR, Ding C, Tang J, et al. Experimental and modeling
740 investigations of ball-milled biochar for the removal of aqueous methylene blue. *Chemical*
741 *Engineering Journal* 2018; 335: 110-119.
- 742 Mandal A, Singh N, Purakayastha T. Characterization of pesticide sorption behaviour of slow
743 pyrolysis biochars as low cost adsorbent for atrazine and imidacloprid removal. *Science of*
744 *the Total Environment* 2017; 577: 376-385.
- 745 Månsson N, Sörme L, Wahlberg C, Bergbäck B. Sources of alkylphenols and alkylphenol ethoxylates
746 in wastewater—a substance flow analysis in Stockholm, Sweden. *Water, Air, & Soil*
747 *Pollution: Focus* 2008; 8: 445-456.
- 748 McBeath AV, Smernik RJ, Schneider MPW, Schmidt MWI, Plant EL. Determination of the
749 aromaticity and the degree of aromatic condensation of a thermosequence of wood charcoal
750 using NMR. *Organic Geochemistry* 2011; 42: 1194-1202.
- 751 Moulder JF, Stickle WF, Sobol PE, Bomben KD. Handbook of X-ray photoelectron spectroscopy.
752 Eden Prairie, Minnesota, USA: Perkin-Elmer Corporation, 1992.
- 753 Niasar HS, Li H, Kasanneni TVR, Ray MB, Xu C. Surface amination of activated carbon and
754 petroleum coke for the removal of naphthenic acids and treatment of oil sands process-
755 affected water (OSPW). *Chemical Engineering Journal* 2016; 293: 189-199.

- 756 Ok YS, Tsang DC, Bolan N, Novak JM. Biochar from Biomass and Waste: Fundamentals and
757 Applications: Elsevier, 2018.
- 758 OSPAR Commision. Background Document on nonylphenol/nonylphenol ethoxylates, 2009.
- 759 Peiris C, Gunatilake SR, Mlsna TE, Mohan D, Vithanage M. Biochar based removal of antibiotic
760 sulfonamides and tetracyclines in aquatic environments: a critical review. Bioresource
761 Technology 2017.
- 762 Prasanta J, Bruzzoniti MC, Appendini M, Rivoira L, Del Bubba M, Rossini D, et al. Processing of
763 polymer-derived silicon carbide foams and their adsorption capacity for non-steroidal anti-
764 inflammatory drugs. Ceramics International 2016; 42: 18937-18943.
- 765 Reguyal F, Sarmah AK. Adsorption of sulfamethoxazole by magnetic biochar: Effects of pH, ionic
766 strength, natural organic matter and 17 α -ethinylestradiol. Science of the Total Environment
767 2018; 628: 722-730.
- 768 Rivoira L, Appendini M, Fiorilli S, Onida B, Del Bubba M, Bruzzoniti MC. Functionalized iron
769 oxide/SBA-15 sorbent: investigation of adsorption performance towards glyphosate
770 herbicide. Environmental Science and Pollution Research 2016; 23: 21682-21691.
- 771 Sarkar P, Sahu SG, Mukherjee A, Kumar M, Adak AK, Chakraborty N, et al. Co-combustion studies
772 for potential application of sawdust or its low temperature char as co-fuel with coal. Applied
773 Thermal Engineering 2014; 63: 616-623.
- 774 Shimabuku KK, Kearns JP, Martinez JE, Mahoney RB, Moreno-Vasquez L, Summers RS. Biochar
775 sorbents for sulfamethoxazole removal from surface water, stormwater, and wastewater
776 effluent. Water research 2016; 96: 236-245.
- 777 Sposito G. On the use of the Langmuir equation in the interpretation of “adsorption” phenomena: II.
778 The “two-surface” Langmuir equation 1. Soil Science Society of America Journal 1982; 46:
779 1147-1152.

780 Sun L, Wan S, Luo W. Biochars prepared from anaerobic digestion residue, palm bark, and
781 eucalyptus for adsorption of cationic methylene blue dye: characterization, equilibrium, and
782 kinetic studies. *Bioresource Technology* 2013; 140: 406-413.

783 Sun Y, Yu IKM, Tsang DCW, Cao X, Lin D, Wang L, et al. Multifunctional iron-biochar composites
784 for the removal of potentially toxic elements, inherent cations, and hetero-chloride from
785 hydraulic fracturing wastewater. *Environment International* 2019; 124: 521-532.

786 Tan X-f, Liu S-b, Liu Y-g, Gu Y-l, Zeng G-m, Hu X-j, et al. Biochar as potential sustainable
787 precursors for activated carbon production: Multiple applications in environmental protection
788 and energy storage. *Bioresource Technology* 2017; 227: 359-372.

789 Tan X, Liu Y, Zeng G, Wang X, Hu X, Gu Y, et al. Application of biochar for the removal of
790 pollutants from aqueous solutions. *Chemosphere* 2015; 125: 70-85.

791 The Commission of the European Communities. Implementing Council Directive 96/23/EC
792 concerning the performance of analytical methods and the interpretation of results. *Off J Eur*
793 *Commun.*, 2002.

794 Thermo Fisher Scientific. XPS Elements Table - Carbon. 2019,
795 <https://xpssimplified.com/elements/carbon.php>, accessed on 12 July 2019, 2019a.

796 Thermo Fisher Scientific. XPS Elements Table - Oxygen. 2019,
797 <https://xpssimplified.com/elements/oxygen.php>, accessed on 12 July 2019, 2019b.

798 USEPA. SW-846 Test Method 6020B: inductively coupled plasma - mass spectrometry, part of test
799 methods for evaluating solid waste, physical/chemical methods, Washington, D.C., 2014.

800 Vega-Morales T, Sosa-Ferrera Z, Santana-Rodríguez J. Determination of alkylphenol
801 polyethoxylates, bisphenol-A, 17 α -ethynylestradiol and 17 β -estradiol and its metabolites in
802 sewage samples by SPE and LC/MS/MS. *Journal of Hazardous Materials* 2010; 183: 701-
803 711.

- 804 Wan Z, Sun Y, Tsang DC, Iris K, Fan J, Clark JH, et al. A sustainable biochar catalyst synergized
805 with copper heteroatoms and CO₂ for singlet oxygenation and electron transfer routes. *Green*
806 *Chemistry* 2019; 21: 4800-4814.
- 807 Wang Z, Guo H, Shen F, Yang G, Zhang Y, Zeng Y, et al. Biochar produced from oak sawdust by
808 Lanthanum (La)-involved pyrolysis for adsorption of ammonium (NH₄⁺), nitrate (NO₃⁻),
809 and phosphate (PO₄³⁻). *Chemosphere* 2015; 119: 646-653.
- 810 Xiang Y, Xu Z, Wei Y, Zhou Y, Yang X, Yang Y, et al. Carbon-based materials as adsorbent for
811 antibiotics removal: Mechanisms and influencing factors. *Journal of environmental*
812 *management* 2019; 237: 128-138.
- 813 Xiao F, Pignatello JJ. Interactions of triazine herbicides with biochar: Steric and electronic effects.
814 *water research* 2015; 80: 179-188.
- 815 Ying G-G. Fate, behavior and effects of surfactants and their degradation products in the
816 environment. *Environment international* 2006; 32: 417-431.
- 817 Zhang W, Chang QG, Liu WD, Li BJ, Jiang WX, Fu LJ, et al. Selecting activated carbon for water
818 and wastewater treatability studies. *Environmental Progress & Sustainable Energy* 2007; 26:
819 289-298.
- 820 Zhao L, Cao X, Mašek O, Zimmerman A. Heterogeneity of biochar properties as a function of
821 feedstock sources and production temperatures. *Journal of hazardous materials* 2013; 256: 1-
822 9.
- 823 Zheng H, Zhang Q, Liu G, Luo X, Li F, Zhang Y, et al. Characteristics and mechanisms of
824 chlorpyrifos and chlorpyrifos-methyl adsorption onto biochars: Influence of deashing and low
825 molecular weight organic acid (LMWOA) aging and co-existence. *Science of The Total*
826 *Environment* 2019; 657: 953-962.
- 827 Zheng W, Guo M, Chow T, Bennett DN, Rajagopalan N. Sorption properties of greenwaste biochar
828 for two triazine pesticides. *Journal of Hazardous Materials* 2010; 181: 121-126.

829 Zhu X, Li C, Li J, Xie B, Lü J, Li Y. Thermal treatment of biochar in the air/nitrogen atmosphere for
830 developed mesoporosity and enhanced adsorption to tetracycline. *Bioresource technology*
831 2018; 263: 475-482.
832

Table 1 – Elemental composition of biochars produced at pyrolysis temperatures of 450°C (BC450), 650°C (BC650), 850°C (BC850), vegetal activated carbon (VAC) and mineral activated carbon (MAC). Data are presented as mean (n=3) and standard deviation (in bracket).

Char	C (%)	H (%)	N (%)	S (%)	O (%)
BC450	67.2 (0.1)	2.7 (0.2)	0.1071 (0.0003)	< 0.05 ^a	27.8 (0.2)
BC650	80.0 (0.3)	2.1 (0.1)	0.086 (0.008)	< 0.05 ^a	16.1 (0.2)
BC850	82.7 (0.3)	1.3 (0.4)	0.070 (0.01)	< 0.05 ^a	13.6 (0.7)
VAC	90.2 (0.4)	0.55 (0.05)	0.097 (0.002)	< 0.05 ^a	7.0 (0.4)
MAC	77.66 (0.07)	1.21 (0.08)	0.235 (0.002)	0.64 (0.01)	12.2 (0.1)

^aDetection limit.

Table 2 – Total surface area (BET method), surface area of micropores (t-plot method) and surface area of mesopores (BJH model – desorption cumulative surface area) determined in biochars produced by pyrolysis at 450 °C (BC450), 650 °C (BC650) and 850 °C (BC850), and in vegetal and mineral commercial activated carbons (VAC and MAC, respectively). Values of total surface area in bracket represent the instrumental standard deviation.

	Total Surface Area (m² g⁻¹)	Micropore Surface Area (m² g⁻¹)	Mesopore Surface Area (m² g⁻¹)
BC450	102 (4)	73.9	20.9
BC650	319 (13)	253.4	28.9
BC850	419 (16)	296.4	80.8
VAC	785 (30)	474.6	192.0
MAC	1105 (34)	122.0	637.0

Table 3 – Mean values (n=3) and standard deviations (in brackets) of water-extractable metals in biochars and mineral activated carbon. Values are compared with those reported in the European Regulation EN 12915-1/2009.

Metal	Unit	Blank	BC450	BC650	BC850	MAC	EN 12915-1
As	µg L ⁻¹	<0.5 ^a	<0.5 ^a	<0.5 ^a	<0.5 ^a	11 (1)	10
Cd	µg L ⁻¹	<0.5 ^a	<0.5 ^a	<0.5 ^a	<0.5 ^a	<0.5 ^a	0.5
Cr	µg L ⁻¹	<0.5 ^a	0.6 (0.1)	0.5 (0.1)	1.0 (0.1)	<0.5 ^a	5
Hg	µg L ⁻¹	<0.1 ^a	<0.1 ^a	<0.1 ^a	<0.1 ^a	<0.1 ^a	0.3
Ni	µg L ⁻¹	<0.5 ^a	2.2 (0.3)	<0.5 ^a	1.4 (0.2)	1.3 (0.1)	15
Pb	µg L ⁻¹	<0.5 ^a	<0.5 ^a	<0.5 ^a	<0.5 ^a	<0.5 ^a	5
Sb	µg L ⁻¹	<0.5 ^a	<0.5 ^a	<0.5 ^a	<0.5 ^a	1.2 (0.1)	3
Se	µg L ⁻¹	<0.5 ^a	<0.5 ^a	<0.5 ^a	<0.5 ^a	<0.5 ^a	3
Al	µg L ⁻¹	8.1 (1.0)	7.5 (0.7)	28 (3)	232 (15)	207 (16)	n.s.
Fe	µg L ⁻¹	<5 ^a	<5 ^a	8.0 (1.1)	12 (2)	<5 ^a	n.s.
Mn	µg L ⁻¹	3.2 (0.1)	37 (3)	34 (5)	21 (1)	3.4 (0.2)	n.s.
Cu	mg L ⁻¹	<0.005 ^a	<0.005 ^a	<0.005 ^a	<0.005 ^a	<0.005 ^a	n.s.
V	µg L ⁻¹	<0.5 ^a	<0.5 ^a	<0.5 ^a	<0.5 ^a	1.4 (0.1)	n.s.
Zn	µg L ⁻¹	12 (2)	35 (5)	16 (3)	21 (2)	10 (2)	n.s.
B	mg L ⁻¹	0.02 (0.01)	0.05 (0.01)	0.04 (0.01)	<0.01 ^a	<0.01 ^a	n.s.
Na	mg L ⁻¹	12 (1)	13 (1)	11 (2)	11 (1)	11 (1)	n.s.
K	mg L ⁻¹	<0.3 ^a	5.2 (1.0)	3.3 (0.7)	4.2 (0.3)	1.5 (0.3)	n.s.
Mg	mg L ⁻¹	5.0 (0.8)	4.3 (0.4)	5.2 (0.8)	5.5 (0.61)	4.1 (0.5)	n.s.
Ca	mg L ⁻¹	12 (2)	11 (1)	18 (3)	19 (2)	12 (1)	n.s.
Ba	µg L ⁻¹	<10 ^a	60 (3)	46 (2)	63 (5)	12 (1)	n.s.

^aMDLs = method detection limits at signal-to-noise ratio of 3; n.s. = not specified.

Table 4 – Mean concentration values (ng L⁻¹, n=3) and standard deviations (in brackets) of water-extractable PAHs in biochars and mineral activated carbon.

Compound	BC450	BC650	BC850	MAC
Naphthalene	0.67 (0.02)	0.40 (0.01)	n.d.	n.d.
Acenaphthene	0.38 (0.01)	<MQL	n.d.	n.d.
Acenaphthylene	0.48 (0.01)	<MQL	n.d.	n.d.
Fluorene	0.35 (0.01)	<MQL	n.d.	n.d.
Phenanthrene	7.0 (0.3)	2.92 (0.06)	1.28 (0.05)	2.24 (0.09)
Anthracene	0.35 (0.01)	n.d.	n.d.	n.d.
Fluoranthene*	0.53 (0.02)	0.33 (0.01)	0.23 (0.01)	0.50 (0.02)
Pyrene	0.34 (0.01)	<MQL	MQL	2.7 (0.1)
Benzo(a)anthracene	2.2 (0.1)	1.03 (0.05)	n.d.	n.d.
Chrysene	2.05 (0.09)	1.71 (0.08)	n.d.	n.d.
Benzo(b)fluoranthene*	0.79 (0.04)	MDL	n.d.	n.d.
Benzo(k)fluoranthene*	0.64 (0.03)	MDL	n.d.	n.d.
Benzo(a)pyrene*	0.89 (0.05)	MDL	n.d.	n.d.
Benzo(a,h)anthracene	2.0 (0.1)	1.51 (0.08)	n.d.	n.d.
Indeno(1,2,3-c,d)pyrene*	2.4 (0.1)	1.8 (0.1)	n.d.	n.d.
Benzo(g,h,i)perylene*	1.66 (0.09)	1.05 (0.06)	n.d.	n.d.
Sum*	6.91	3.18	0.23	0.50

(*) Compounds regulated as sum in the EN 12915-1/2009. Maximum acceptable total concentration = 20 ng L⁻¹; n.d. = not detected. MDL = method detection limit; MQL = method quantification limit.

Table 5 – Mean (n=3) and standard deviations (in brackets) of Freundlich adsorption capacity (K_F), calculated for biochars (BC450, BC650 and BC850) and mineral activated carbon (MAC) in the ranges 5–400 $\mu\text{g L}^{-1}$ for AP_nEO technical mixtures, and in the ranges 0.5–40 $\mu\text{g L}^{-1}$ for APs. Different letters within each line means statistically significant differences according to the Games-Howell non-parametric contrast test (P<0.05)

Analyte	K_F			
	BC450	BC650	BC850	MAC
4-t-OP	0.563 (0.008) a	1.05 (0.05) b	0.63 (0.02) a	9.4 (0.5) c
4-t-OP ₂ EO	0.40 (0.04) a	0.48 (0.02) a	0.586 (0.004) b	8.38 (0.08) c
4-t-OP ₃ EO	0.48 (0.06) a	0.53 (0.01) a	0.72 (0.01) b	10.0 (0.2) c
4-t-OP ₄ EO	0.50 (0.06) ab	0.442 (0.007) a	0.70 (0.02) b	9.9 (0.2) c
4-t-OP ₅ EO	0.42 (0.05) a	0.528 (0.002) a	0.63 (0.02) b	8.8 (0.2) c
4-t-OP ₆ EO	0.36 (0.04) ab	0.43 (0.01) a	0.464 (0.005) b	7.4 (0.2) c
4-t-OP ₇ EO	0.211 (0.008) a	0.214 (0.006) a	0.212 (0.006) a	6.1 (0.2) b
4-t-OP ₈ EO	0.166 (0.003) a	0.218 (0.006) b	0.213 (0.005) b	4.5 (0.2) c
4-NP	1.5 (0.2) a	2.07 (0.01) b	1.07 (0.04) a	26.2 (0.6) c
4-NP ₂ EO	0.84 (0.03) a	1.23 (0.03) b	1.11 (0.03) c	22.0 (0.4) d
4-NP ₃ EO	0.99 (0.08) ab	1.12 (0.04) a	0.79 (0.01) b	21.1 (0.2) c
4-NP ₄ EO	1.00 (0.07) ab	1.12 (0.03) a	0.712 (0.004) b	19.2 (0.2) c
4-NP ₅ EO	0.9 (0.2) a	0.870 (0.007) a	0.834 (0.004) a	15.98 (0.06) b
4-NP ₆ EO	0.52 (0.03) ab	0.619 (0.001) a	0.583 (0.008) b	12.9 (0.1) c
4-NP ₇ EO	0.44 (0.02) a	0.397 (0.003) a	0.375 (0.003) b	10.82 (0.04) c
4-NP ₈ EO	0.33 (0.02) ab	0.377 (0.002) a	0.366 (0.003) b	8.6 (0.2) c

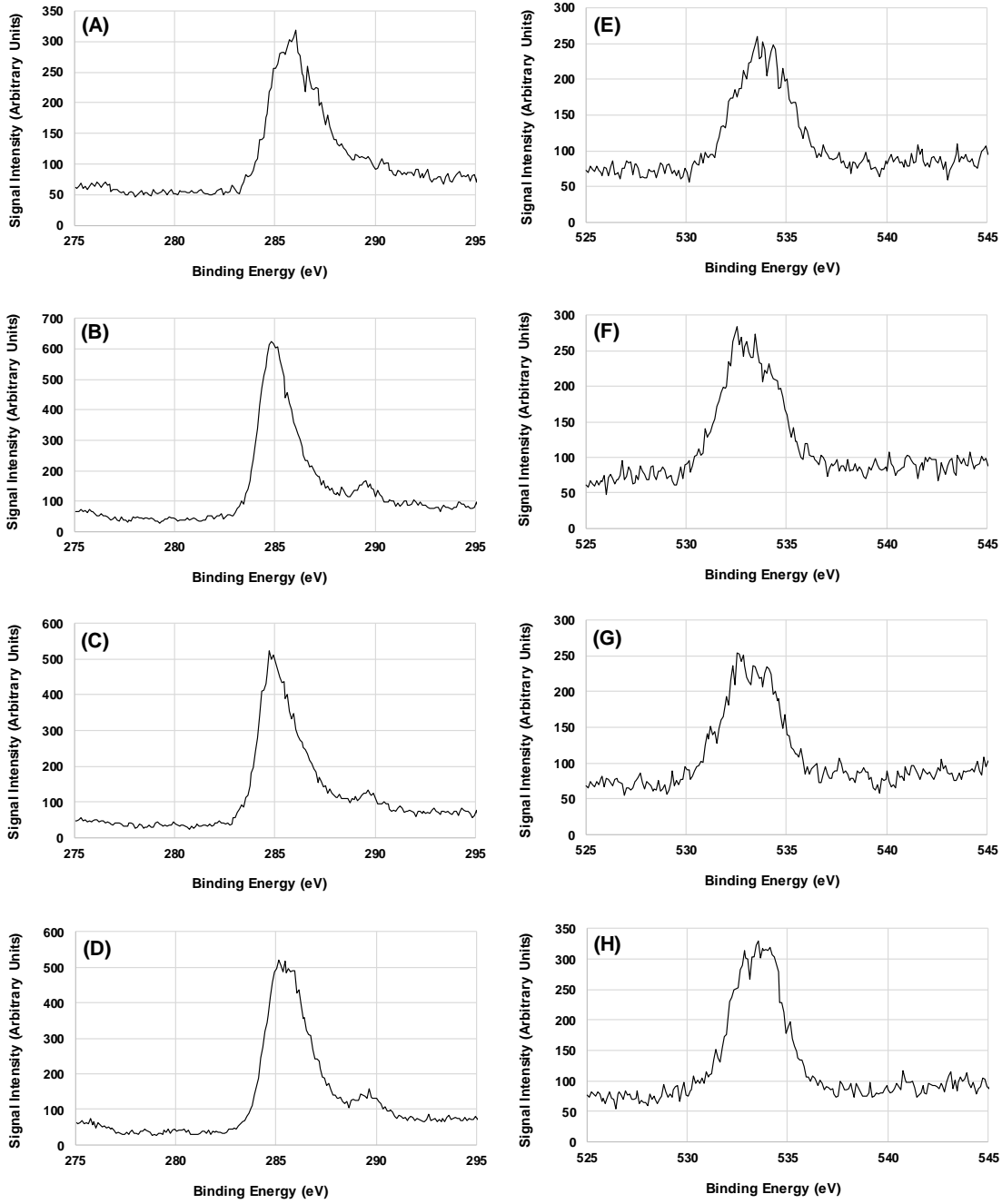


Figure 1 – X-ray photoelectron spectroscopy spectra in the binding energy regions of carbon (A-D) and oxygen (E-H) of biochars produced by pyrolysis at 450 °C (A, E), 650 °C (B, F) and 850 °C (C, G), and of mineral commercial activated carbon (D, H).

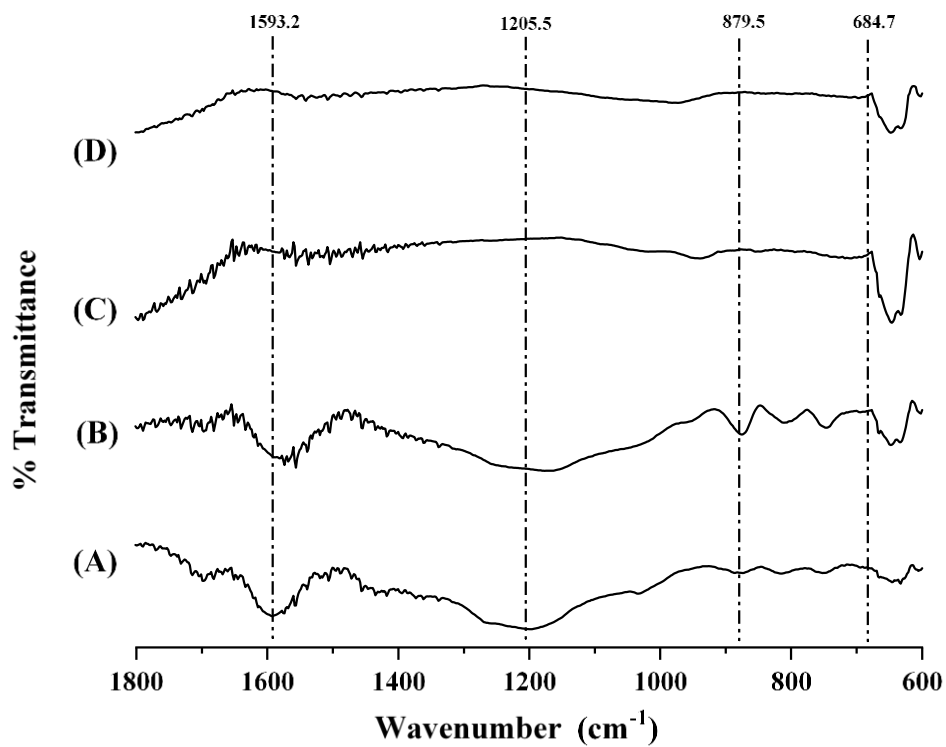


Figure 2 – Fourier-transform infrared spectra of biochars produced by pyrolysis at 450 °C (A), 650 °C (B) and 850 °C (C), and of mineral commercial activated carbon (D).

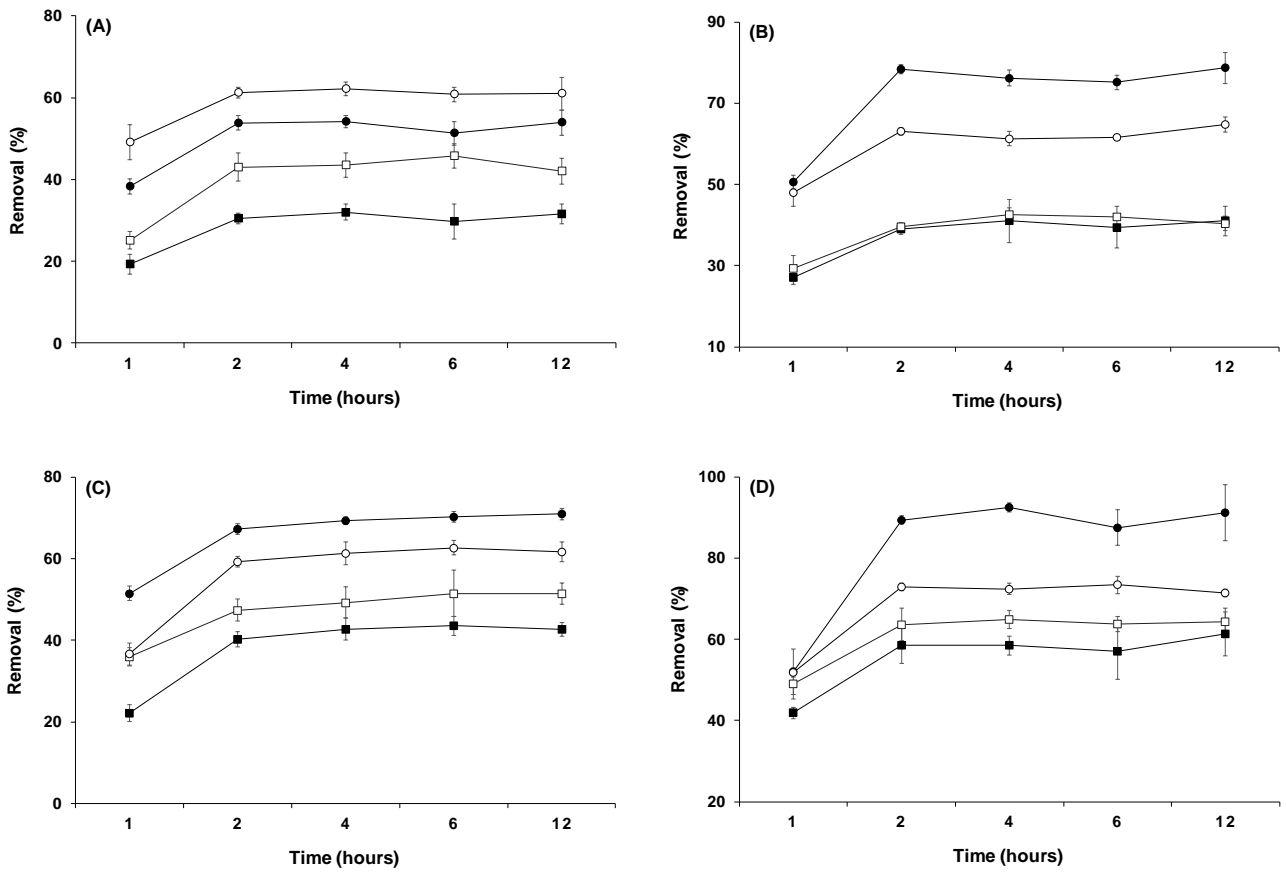


Figure 3 – Removal of 4-t-OP (■), 4-t-OP₈EO (□), 4-NP (●) and 4-NP₈EO (○) at contact times of 1, 2, 4, 6 and 12 hours, provided by BC450 (A), BC650 (B), BC850 (C) and MAC (D). Concentrations of biochars = 10 mg L⁻¹; concentration of MAC = 1 mg L⁻¹. Concentrations of 4-t-OP, 4-NP and of technical mixtures containing 4-t-OP₈EO and 4-NP₈EO = 400 µg L⁻¹. Error bars represent standard deviations (n=3).

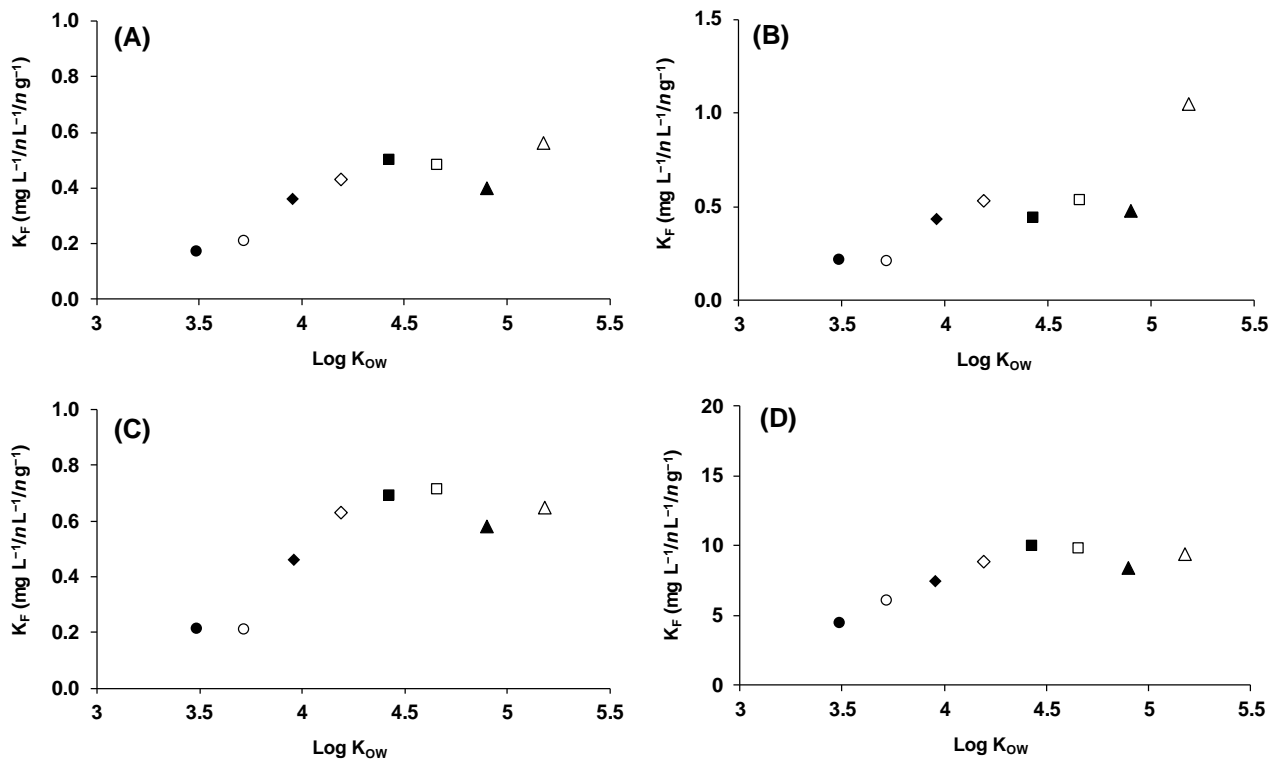


Figure 4 – Trend of Freundlich adsorption capacity (K_F) as a function of $\log K_{OW}$ values for: 4-t-OP₈EO (●); 4-t-OP₇EO (○); 4-t-OP₆EO (◆); 4-t-OP₅EO (◇); 4-t-OP₄EO (■); 4-t-OP₃EO (□); 4-t-OP₂EO (▲); 4-t-OP (△). (A) BC450; (B) BC650; (C) BC850 and (D) MAC.

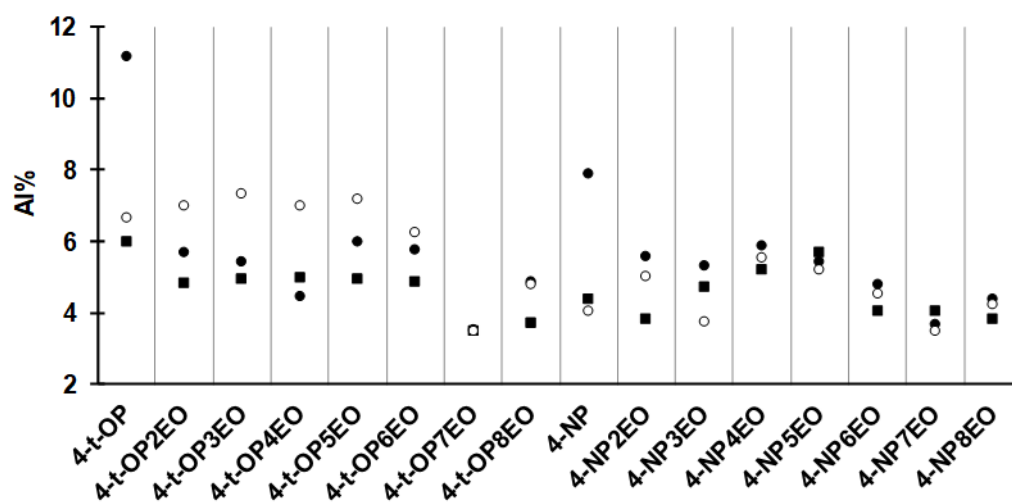


Fig. 5 – Mean values of relative adsorption index (AI%) determined for each target analyte, expressed as the percentage ratio between K_F values for a biochar and the virgin mineral activated carbon. BC450 (■); BC650 (●); BC850 (○).

Supplementary material of the Manuscript: “Physicochemical properties and sorption capacities of sawdust-based biochars and commercial activated carbons towards ethoxylated alkylphenols and their phenolic metabolites in effluent wastewater from a textile district”, by Massimo Del Bubba et al.

S.1 Reagents, standards and materials

Hydrochloric acid, phosphoric acid, methylene blue tri-hydrate and dichloromethane were purchased from Carlo Erba Reagents (Cornaredo, Milano, Italy). Phenol, sodium bicarbonate, calcium chloride, magnesium sulphate and isopropyl alcohol were obtained from Sigma-Aldrich (St. Louis, MO, USA). Disodium hydrogen phosphate anhydrous was supplied by Panreac Quimica (Castellar del Vallès, Barcelona, Spain). Acetic acid was purchased from Romil (Waterbeach, Cambridge, UK). Reagent grade sodium thiosulfate and iodine were obtained from Labochimica (Campodarsego, Padova, Italy). Concentrated nitric acid 70%, hydrogen peroxide 30% (trace metal analysis) and all standards (ICP-MS analysis grade) of elements investigated in the chars were supplied from Sigma-Aldrich.

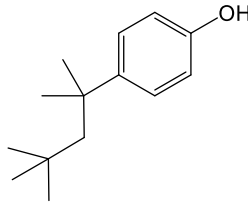
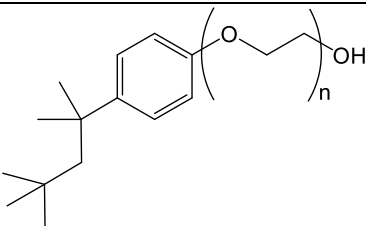
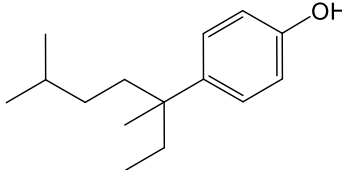
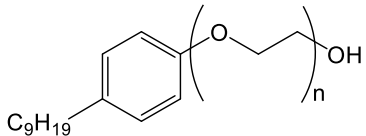
LC-MS grade methanol (CH₃OH), water and ammonia (NH₃ content >25%) were purchased from Sigma-Aldrich. Ultrapure water (resistivity > 18 MΩ) was obtained from a Milli-Q system (Millipore, Billerica, MA, USA).

EPA 610 PAH mixture (Supelco, St. Louis, MO, USA), containing the following polycyclic aromatic hydrocarbons: naphthalene (N), acenaphthene (Acy), acenaphthylene (Ac), fluorene (Fl), anthracene (A), phenanthrene (P), fluoranthene (Flu), pyrene (Py), benzo(a)anthracene (BaA), chrysene (Ch), benzo(b)fluoranthene (BbFlu), benzo(k)fluoranthene (BkFlu), benzo(a)pyrene (BaPy), dibenzo(a,h)anthracene (BahA), indeno(1,2,3-cd)pyrene (Ipy) and benzo(ghi)perylene (BP), was employed. Naphthalene d-8 (N-d8), phenanthrene d-10 (P-d10), fluoranthene d-10 (Flu-d10), chrysene d-12 (Ch-d12), benzo(a)pyrene d-12 (BaPy-d12) and indeno(1,2,3-cd)pyrene d-12 (Ipy-d12) were purchased from Supelco. Reference standards of 4-tert-octylphenol (4-t-OP, purity 97 %, CAS: 140-66-9) and 4-(1-ethyl-1,4-dimethylpentyl)-phenol (4-NP, purity 99.9 %, CAS 142731-63-

3) were obtained from Sigma-Aldrich. Since individual OP_nEO and NP_nEO with n>2 are unavailable as analytical standards, Triton™ X-45 and IGEPAL® CO-520 technical mixtures, purchased from Sigma-Aldrich, have been employed as reference standards of the two AP_nEO classes. These mixtures, respectively consisting of oligomers of 4-t-octylphenol polyethoxylates (4-t-OP_nEOs, with n=1–11) and 4-nonylphenol polyethoxylates (4-NP_nEOs, with n=2–8), were previously characterized by our team (see the reference [11] in the main text). According to this characterization, the relative percentages of the oligomers considered in this study (n=2–8) due to their much larger abundance, were the following. Triton™ X-45: n=2 – 14.3%; n=3 – 22.4%; n=4 – 21.9%; n=5 – 16.0%; n=6 – 10.5%; n=7 – 6.5%; n=8 – 3.6%. IGEPAL® CO-520: n=2 – 14.6%; n=3 – 18.3%; n=4 – 17.7%; n=5 – 14.4%; n=6 – 11.0%; n=7 – 7.9%; n=8 – 5.3%. Stock solutions of Triton™X-45 and IGEPAL® CO-520 (1 mg mL⁻¹) and APs (100 µg mL⁻¹) were prepared in LC–MS grade methanol and then stored in the dark at –20 °C. CAS numbers, structure formulas and Log K_{ow} values of the investigated APs and AP_nEOs are shown in **Table S1**.

The GC column employed for PAH evaluation was an SLB®-5ms fused silica capillary (10 m × 0.10 mm, 0.10 µm film thickness) from Supelco. The SPE cartridge used for the evaluation of polycyclic aromatic hydrocarbons contents in char was the cartridge Strata C18-E (500 mg, 6 mL, 55 µm, 70 Å) from Phenomenex (Torrance, CA, USA). A LC pellicular column Kinetex® Biphenyl (Phenomenex, 100 mm × 3 mm, 2.6 µm particle size), was used for the evaluation of the removal of target compounds by biochars and activated carbon.

Table S1 – Compound names and acronyms (in bracket), CAS, structure formulas and log K_{ow} values of target analytes.

Compound Name	CAS	Structure formula	Log K_{ow} ^a
4-tert-Octylphenol (4-t-OP)	140-66-9		5.18
TRITON™X-45 (4-t-OP _n EO) Technical Mixture of 4-tert-octylphenolpolyethoxylate oligomers with ethoxylation number (n) equal to 2-8.	9002-93-1		3.49-4.90 ^b
4-(1-Ethyl-1,4-dimethylpentyl)-phenol (4-NP)	142731-63-3		5.79
IGEPAL®CO-520 (4-NP _n EO) Technical Mixture of branched 4-nonylphenolpolyethoxylate oligomers with ethoxylation number (n) equal to 2-8.	68412-54-4		4.26-5.50 ^c

^a Calculated using Advanced Chemistry Development (ACD/Labs) Software V11.02 (© 1994-2015 ACD/Labs). ^b Log K_{ow} range of 4-t-OP_nEO oligomers with n=2-8. ^c Log K_{ow} range of 4-NP_nEO oligomers with n=2-8 (when log K_{ow} of the branched oligomer was not available, the value concerning the corresponding compound with linear alkyl chain was reported).

S.2 Characteristics of the effluent wastewater

The effluent wastewater used in this study was obtained from the Baciacavallo WWTP operating in the textile industrial district of Prato (Italy). The wastewater was characterized for the following parameters: pH, total suspended solids (TSS), chemical oxygen demand (COD), five-days biological oxygen demand (BOD₅), total nitrogen (N_{tot}), N-NH₄⁺, N-NO₃⁻, total phosphorus (P_{tot}), Cl⁻, SO₄²⁻, total hardness, total anionic surfactants (MBAS), total cationic surfactants (BiAS), and total surfactants. The characteristics of wastewater are shown in **Table S2**.

Table S2 – Characteristics of the effluent wastewater used in this study. Values are mean of three determinations with corresponding standard deviations in bracket.

Parameter	Value
pH	7.46 (0.04)
TSS (mg/L)	1.1 (0.3)
COD (mg/L)	21 (4)
BOD ₅ (mg/L)	<5
N _{tot} (mg/L)	10.8 (0.2)
N-NH ₄ ⁺ (mg/L)	1.5 (0.4)
N-NO ₃ ⁻ (mg/L)	7.6 (0.5)
P _{tot} (mg/L)	0.7 (0.1)
Cl ⁻ (mg/L)	687 (21)
SO ₄ ²⁻ (mg/L)	224 (18)
Total hardness (mg CaCO ₃ /L)	330 (11)
MBAS (mg/L)	0.21 (0.05)
BiAS (mg/L)	0.07 (0.01)
Total surfactants (mg/L)	0.29 (0.04)
4-t-OP (ng/L)	<95
4-t-OP ₂ EO (ng/L)	12 (2)
4-t-OP ₃ EO (ng/L)	10 (2)
4-t-OP ₄ EO (ng/L)	8 (2)
4-t-OP ₅ EO (ng/L)	7 (1)
4-t-OP ₆ EO (ng/L)	6 (1)
4-t-OP ₇ EO (ng/L)	< 5.5
4-t-OP ₈ EO (ng/L)	< 4.5
4-NP (ng/L)	58 (4)
4-NP ₂ EO (ng/L)	49 (5)
4-NP ₃ EO (ng/L)	37 (2)
4-NP ₄ EO (ng/L)	39 (3)
4-NP ₅ EO (ng/L)	31 (2)
4-NP ₆ EO (ng/L)	29 (2)
4-NP ₇ EO (ng/L)	33 (2)
4-NP ₈ EO (ng/L)	24 (2)

S.3 Metal analysis in recycled sawdust

Total Cd, Cr, Hg and Pb content in sawdust samples was determined by ICP-MS analysis, after acidic-oxidant digestion with trace metal grade reagents, using a microwave system ETHOS-1, (MILESTONE S.r.l., Bergamo, Italy) with pulsed-mode emission. Spontaneously dried sawdust (0.5 g) was treated with 2 mL of 30% hydrogen peroxide and 7 ml of 70% nitric acid, using the following microwave program: from ambient temperature to 180 °C in 10 min, and then isotherm at 180 °C for 10 min. After digestion, sawdust samples were taken up to 50 mL with Milli-Q water, filtered on 0.2 µm pore size PTFE filters, spiked with 1% Au 1000 mg L⁻¹ solution and finally analysed by ICP-MS model 7700X (Agilent Technologies, Santa Clara, CA, U.S.A.) under the following experimental conditions: (i) plasma RF power 1450W, (ii) plasma gas flow (Ar) 15 L min⁻¹ and (iii) auxiliary gas flow (Ar) 1.03 L min⁻¹. Total analysis time, including washing procedure of the system, was about 5 minutes. The entire procedure is programmed and automatically controlled by the MassHunter Workstation software for ICP-MS G7201B ver. B01.02 Build 349.8 patch 2 (Agilent Technologies). For Cr(VI) analysis, 0.5 g of spontaneously dried sawdust were treated with 50 mL of a 0.01 M Na₃PO₄ solution (pH = 11.7) and heated for 5 min at 100 °C. The mixture was filtered through a 0.22 µm nylon membrane and injected for ion chromatographic analysis, which was performed with a Dionex 4000i (Dionex ThermoFisher, Sunnyvale, CA, USA) equipped with a spectrophotometric detector. Dionex IonPac column (AS7, 250 × 4.0 mm) and guard column (AG7, 50 × 4.0 mm) were used. The eluent, 250 mM (NH₄)₂SO₄ and 100 mM NH₄OH (pH 8.8), was delivered at 1 mL/min flow rate. Injection volume was 1000 µL. Detection was performed at 530 nm after post-column derivatization (750 µL reaction coil) with a 0.5 M H₂SO₄ solution with 2 mM DPC (10% CH₃OH). The flow rate of post-column reagent was 0.33 mL/min. Cr(VI) quantification was made by the standard addition method. The sawdust water content, measured by heating the material at 105°C for 1 h, together with the concentrations of selected toxic heavy-metals are shown in **Table S3**.

Table S3 – Water content (%) and concentrations (mg kg⁻¹) of some toxic heavy-metals in recycled sawdust used for biochar production.

Parameter	Value
Water	9.1
Hg	<0.015 ^a
Cd	1.1
Pb	0.9
Hexavalent Cr	<0.020 ^a
Total Cr	1.3

^a quantification limit

S.4 Char characterization

S.4.1 Elemental analysis

Aliquots of about 2 mg of finely grinded samples, dried at 120 °C for 24 hours, were analysed in triplicate using a FlashEA® 1112 elemental analyser Thermo Fisher Scientific (Waltham, MA) equipped with a thermal conductivity detector. The percentage content of oxygen was determined by difference as follows: O(%) = 100 – (C% + H% + N% + S% + ash%). Figure S1 illustrates the van Krevelen diagram of O/C vs H/C ratios.

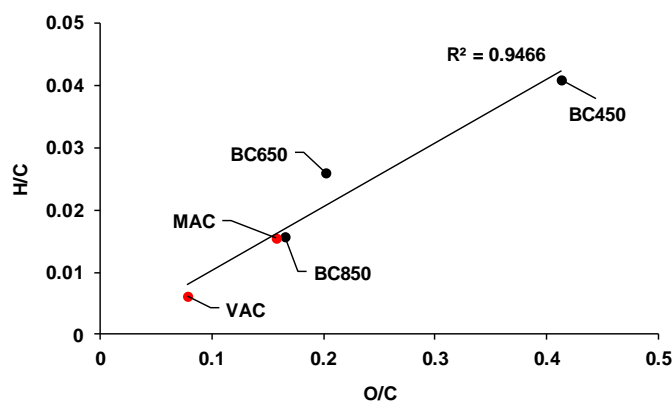


Figure S1 – van Krevelen diagram for vegetal and mineral activated carbons (VAC and MAC, red points), and biochars produced at 450°C (BC450), 650°C (BC650), and 850°C (BC850) (black points).

S.4.2 Physisorption analyses

The textural properties of the biochars obtained at 450 °C (BC450), 650 °C (BC650) and 850 °C (BC850) and of commercial vegetal and mineral activated carbons (VAC and MAC) were determined

by nitrogen adsorption and desorption experiments at -196°C using a Porosity Analyser Micrometrics (Norcross, GA, USA) model ASAP 2020. The surface area was calculated by using the Brunauer-Emmet-Teller (BET) and the Langmuir methods applied to nitrogen adsorption data in the relative pressure (P/P°) range of 0.06-0.40. The total pore volume was determined from the amount of nitrogen adsorbed at $P/P^{\circ}=0.98$. The mesopore size distribution was determined by the Barret-Joyner-Halenda (BJH) model applied to desorption data and the assessment of microporosity was carried out by the t-plot method. For the porosimetry of biochars, a minimum equilibrium interval of 30 s with a maximum relative tolerance of 5% of the targeted pressure and an absolute tolerance of 5 mmHg were used. Before analysis, biochars were activated *in situ*, by heating at 300°C , at a rate of $5^{\circ}\text{C min}^{-1}$, under a high vacuum ($<10^{-8}$ mbar) for 12 h, provided by an oil sealed mechanical vacuum pump coupled with a high vacuum system. For the porosimetry of VAC and MAC a minimum equilibrium interval of 10 s with a maximum relative tolerance of 2% of the targeted pressure and an absolute tolerance of 2 mmHg were adopted. Activated Carbon were activated *in situ* by heating at 200°C , at a rate of $10^{\circ}\text{C min}^{-1}$, under high vacuum for 18 h (same vacuum conditions specified above). Full porosimetry data are illustrated in **Table S4**.

Table S4 – Total surface area (BET and Langmuir methods), surface area of micropores (t-plot method) and mesopores (BJH model – desorption cumulative surface area), total pore volume, micropore (t-plot method) and mesopore volume (BJH model – desorption cumulative volume), average pore width (BJH model – desorption pore width) of biochars obtained by pyrolysis at 450°C (BC450), 650°C (BC650) and 850°C (BC850), and vegetal (VAC) and mineral (MAC) activated carbons.

	Surface Area ($\text{m}^2 \text{g}^{-1}$)				Pore Volume ($\text{cm}^3 \text{g}^{-1}$)			Pore Width (nm)
	BET	Langmuir	t-Plot	BJH	Total	t-plot	BJH	
BC450	102	172	73.9	20.9	0.082	0.045	0.053	9.97
BC650	319	536	253.4	28.9	0.194	0.154	0.024	3.32
BC850	419	710	296.4	80.8	0.267	0.183	0.071	3.52
VAC	785	1333	474.6	192.0	0.555	0.302	0.223	4.74
MAC	1105	1967	122.0	637.0	0.767	0.133	0.513	3.22

S.4.3 Porosity indexes and ash content

Porosity indexes and ash content were measured following official methods of analysis of activated carbon, as specified in the main text of the manuscript. The results of these characterizations are shown in **Table S5**.

Table S5 – Mean values (n=3) and standard deviations (in brackets) of porosity indexes and ash percentage determined in each investigated char.

Char	Iodine index	Phenol index	Methylene blue index	Ash
BC450	102 (1)	18.9 (0.9)	2.2 (0.1)	2.11 (0.05)
BC650	157 (8)	9.5 (0.2)	2.9 (0.1)	1.74 (0.03)
BC850	190 (4)	2.4 (0.1)	3.6 (0.2)	2.30 (0.02)
VAC	964 (10)	1.9 (0.1)	16.6 (0.2)	2.13 (0.04)
MAC	1192 (9)	1.4 (0.1)	20.0 (0.1)	8.02 (0.03)

In **Figure S2** adsorption indexes are plotted as a function of BET surface area (**Fig. S2A-C**) and micropore (**Fig. S2D-E**) and mesopore (**Fig. S2F**) surface area.

S.4.4 pH of the point of zero charge

The pH of the point of zero charge (pH_{pzc}) of biochars and MAC was determined using the pH drift method using the following procedure. Stock solutions of 0.1 M NaCl were prepared at pH 2, 3, 4, 5, 6, 7, 8, 9, 10, and 11 (pH_i) by adding 1 M NaOH or 1 M HCl. Aliquots of 50 mL of these solutions were then transferred to a series of volumetric flasks and 0.1 g of each sorbent was added. The flasks were sealed and the suspensions orbital shaken at 150 rpm for 32 h before the final pH value (pH_f) of the supernatant was recorded. The difference between pH_i and pH_f (Δ pH) was plotted as a function of pH_i, and the point of the intersection of the resulting curve with pH_i axis was pH_{pzc}. The results are illustrated in **Figure S3**.

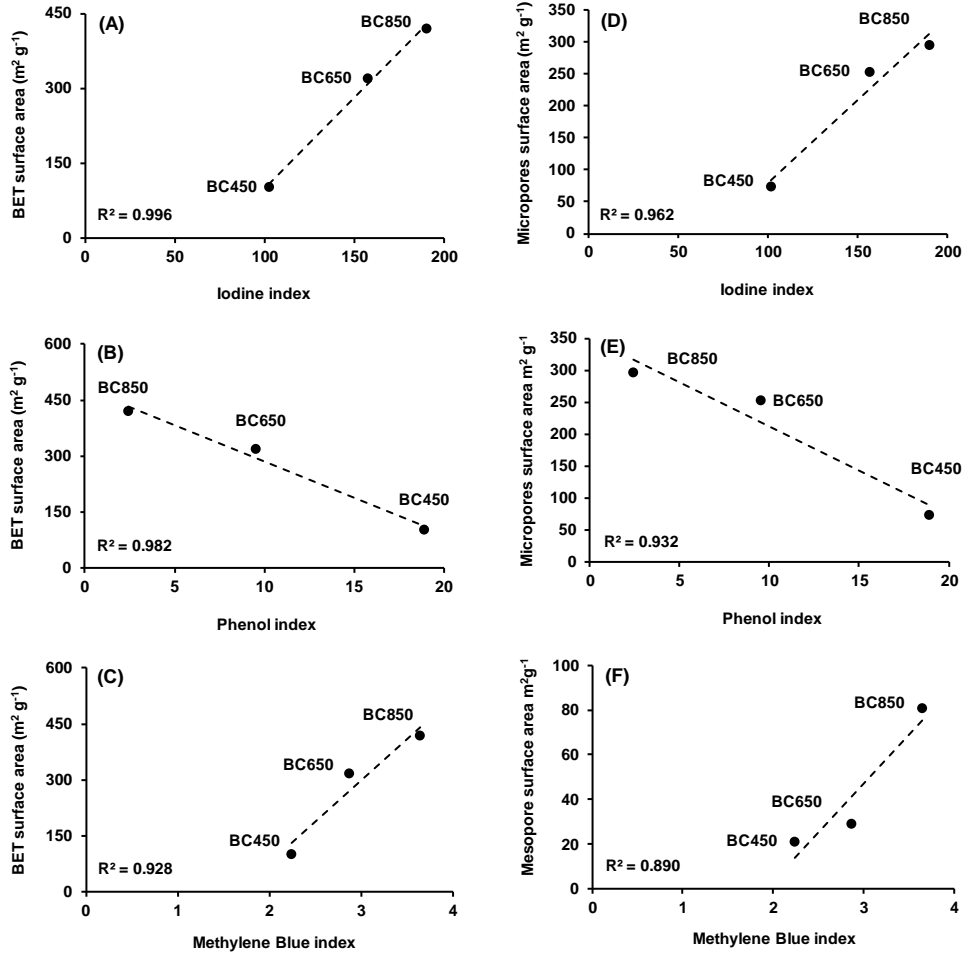


Figure S2 – Plots of BET surface areas (A-C), t-plot micropore surface areas (D-E) and BJH mesopore surface area (F) as a function of porosity indexes determined in BC450, BC650 and BC850. Values of determination coefficients (R^2) are reported in the plots.

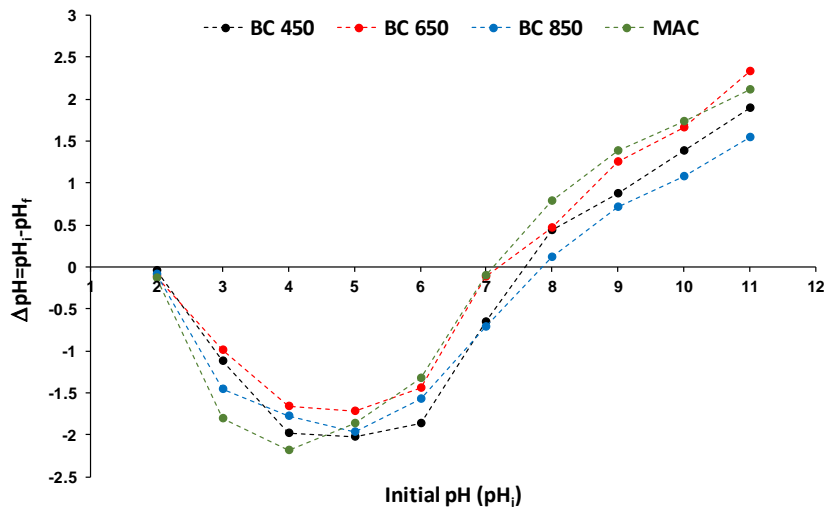


Figure S3 – Point of zero charge of biochars produced by pyrolysis at 450 °C (BC450), 650 °C (BC650) and 850 °C (BC850), and of commercial mineral activated carbon (MAC).

S.4.5 X-ray photoelectron spectroscopy (XPS) analysis

The chemical compositions of the near surface sample portions of BC450, BC650, BC850 and MAC were obtained by means of XPS experiments carried out in an ultrahigh vacuum (UHV, 10^{-9} mbar) system equipped with a VSW HAC 500 hemispherical electron-energy analyzer using a non-monochromatic Mg K-alpha X-ray source operating at 120 W power (10 kVx10 mA). The samples were fixed to the sample holder by means of a conductive carbon tape and introduced in the UHV under an inert gas (N_2) flux. Survey and high-resolution spectra were acquired in the constant analyzer energy mode (CAE) at pass energy of 22 eV with a step size of 1.0 and 0.1 eV, respectively. The peaks were fitted using CasaXPS software employing Gauss-Lorentz curves after subtraction of a Shirley-type background. Peak areas experimentally obtained were corrected using sensitivity factors of 0.296 and 0.711, for C and O, respectively (**Table S6**). These indexes referred to fluorine, the sensitivity factor of which is taken equal to 1.000, considering an x-ray source located at 54.7° relative to the analyser axis.

Table S6 – Experimental and corrected XPS areas, and relative percentages of carbon and oxygen determined in biochars produced at pyrolysis temperatures of 450°C (BC450), 650°C (BC650), 850°C (BC850), and in mineral activated carbon (MAC).

Char	C	C _{corrected}	O	O _{corrected}	C (%)	O(%)
BC450	731	2470	548	771	76.2	23.8
BC650	1294	4372	635	893	83.0	17.0
BC850	1195	4037	577	812	83.3	16.7
MAC	1359	4591	791	1113	80.5	19.5

S.5 Water-extractable substances

According to the UNI EN 12902:2004 standard method, 25 grams of char are put in contact with 2.5 L of extraction water and the solution is shaken for 24 hours at 25°C . Extraction water was a NaHCO_3 0.5 mM, CaCl_2 0.3 mM and MgSO_4 0.2 mM aqueous solution ($\text{pH}=7.5\pm 0.2$); Afterwards, the obtained

suspension was filtered on 0.4 μm polycarbonate membranes (Sigma-Aldrich, St. Louis, MO, USA) and divided in two aliquots for metal and PAH analysis.

S.5.1 Analysis of water extractable metals

The filtered water sample (100 mL aliquots) was treated with 1 mL of concentrated nitric acid, spiked with 1% Au 1000 mg L^{-1} solution and directly analysed by an ICP-MS model 7700X (Agilent Technologies, Santa Clara, CA, U.S.A.) under the experimental conditions described in S2.

S.5.2 Analysis of water extractable PAHs

PAHs were analysed according to the following internal method: 2.0 L of filtered solution were spiked with 5 mL of methanol, stirred and then loaded on a C18-SPE cartridge previously conditioned with (i) 4 mL of isopropyl alcohol, (ii) 4 mL of a 15/85 (v/v) isopropyl alcohol/water mixture and (iii) 25 mL of methanol. Afterward, the cartridge was dried under vacuum and the elution of the selected compounds was carried out with 6 mL of dichloromethane. The recovered solution was concentrated under a gentle nitrogen stream to 50 μL and analysed by a Shimadzu (Kyoto, Japan) gas chromatograph model GC2010 equipped with an AOC-20i auto-injector (Shimadzu) and an AOC-20s auto-sampler (Shimadzu) and coupled with a QP2010 Plus mass spectrometer (Shimadzu). The GC column employed was an SLB®-5ms fused silica capillary (10 m \times 0.10 mm, 0.10 μm particle size) from Supelco.

The GC analysis was performed according to the following conditions: (i) 1 μL of sample was injected in splitless mode, (ii) injector temperature: 320°C, (iii) column flow: 1.2 mL min^{-1} and (iv) constant linear velocity: 69.2 cm s^{-1} .

Temperature programme: 60 °C initial temperature for 2 min, from 60°C to 160 °C in 2.2 min, from 160°C to 200°C in 2.0 min, from 200°C to 210°C in 3.3 min, from 210°C to 225° C in 15.0 min. from 255°C to 244°C in 6.3 min, from 240°C to 320°C in 1.9 min, final isotherm for 1.0 min. MS conditions: ion source temperature: 230°C; interface temperature: 280°C; detector voltage: 0.5 kV; analysis mode: single ion monitoring (SIM), see **Table S7** for the complete list of the selected ions.

Instrumental control and data processing were carried out by the GCMS Solution software, version 2.50 (Shimadzu).

The figure of merits of the instrumental method – i.e. limits of detection (IDLs), limits of quantification (IQLs), linearity and precision – obtained by replicated injections of standard solutions in dichloromethane, are shown in **Table S8**. IDLs and IQLs were taken as the minimum concentrations of target analytes that give rise to a signal to noise ratio (S/N) equal to 3 and 10, respectively.

Table S7 – GC-MS retention time (Rt), quantifier and qualifier ions of the investigated PAHs and selected labelled surrogate standards. The meaning of target analyte acronyms is reported in S1.

Compound	Rt [min]	Quantifier ion	Qualifier ion
N	3.5	128	127
Acy	4.4	152	151
Ac	4.5	153	154
Fl	4.9	165	165
P	5.7	178	176
A	5.8	178	176
Flu	7.0	202	200
Py	7.4	202	200
BaA	10.5	228	226
Ch	10.6	228	226
BbFlu	15.8	252	250
BkFlu	16.1	252	250
BaPy	18.0	252	250
Ipy	27.3	276	274
BahA	28.4	278	276
BP	29.8	276	274
N-d8	3.5	136	134
P-d10	5.7	188	184
Flu-d10	7.0	212	208
Ch-d12	10.5	240	236
BaPy-d12	18.0	264	260
Ipy-d12	27.3	288	284

The linearity was investigated by replicated analysis (n=5) of standard solutions from five calibration levels of PAHs. For each analyte concentration ranges were chosen starting from the IQLs up to three magnitude orders expressed as ng injected. Intra-day ($RSD\%_{intra}$) and inter-day ($RSD\%_{inter}$) precision were evaluated by ten replicated injections of standard solutions, at concentration levels twice higher than IQLs.

Table S8 – Instrumental figure of merits of GC-MS analysis of PAHs. The meaning of target analyte acronyms is reported in S1.

Compound	IDL (ng injected)	Linearity range (ng injected)^a	R²	RSD%_{intra}	RSD%_{inter}
N	0.001	0.005 – 52.64	0.9996	2.1	2.8
Acy	0.001	0.004 – 52.98	0.9998	3.3	3.5
Ac	0.001	0.004 – 52.98	0.9994	2.4	2.8
Fl	0.001	0.005 – 5.40	0.9975	3.1	3.5
P	0.002	0.007 – 5.34	0.9996	3.5	3.8
A	0.002	0.007 – 5.37	0.9994	3.7	4.0
Flu	0.001	0.005 – 10.20	0.9994	3.2	3.3
Py	0.001	0.005 – 4.97	0.9987	3.4	3.5
BaA	0.003	0.01 – 26.63	0.9997	4.4	4.5
Ch	0.005	0.02 – 26.63	0.9994	4.2	4.4
BbFlu	0.004	0.015 – 10.87	0.9977	5.3	5.5
BkFlu	0.004	0.015 – 5.39	0.9983	5.1	5.4
BaPy	0.005	0.02 – 27.9	0.9995	4.8	5.2
BahA	0.008	0.03 – 29.16	0.9994	5.2	5.3
Ipy	0.006	0.025 – 26.75	0.9986	5.4	5.5
BP	0.008	0.030 – 3.15	0.9948	5.5	5.6
N-d8	0.001	0.005 – 51.37	0.9998	1.9	2.2
P-d10	0.002	0.007 – 5.52	0.9997	2.7	3.1
Flu-d10	0.001	0.005 – 12.33	0.9995	2.8	3.0
Ch-d12	0.005	0.02 – 24.53	0.9997	3.2	3.5
BaPy-d12	0.005	0.02 – 26.8	0.9993	4.2	4.8
Ipy-d12	0.006	0.02 – 21.15	0.9987	5.1	5.3

^a The lower limits of the linearity ranges represent IQLs.

In order to evaluate the SPE apparent recovery, three 2 L aliquots of extraction water were fortified with labelled compounds (5 ng L⁻¹ for N-d8, P-d10, Flu-d10 and Ch-d12 and 10 ng L⁻¹ for BaP-d12 and Ipy-d12). The spiked samples were subjected to the SPE procedure, followed by the GC-MS analysis; the resulting mean areas (n=3) were compared to the mean areas (n=3) obtained by spiking 50 µL of dichloromethane with the same amounts of mass labelled compounds.

The following deuterated PAHs were used for calculating apparent recoveries: (i) N-d8 for N, (ii) P-d10 or 3-ring PAHs, (iii) Flu-d10 for Flu, (iv) Ch-d12 for 4-ring PAHs, (v) BaP-d12 for 5-ring PAHs and (vi) Ipy-d12 for 6-ring PAHs. The recoveries of mass labelled analytes are detailed in **Figure S4**, and the detection (MDLs) and quantification (MQLs) limits of the whole analytical procedure are shown in **Table S9**. The overall MQLs in extraction water were found in the range of 0.13 – 0.9 ng L⁻¹.

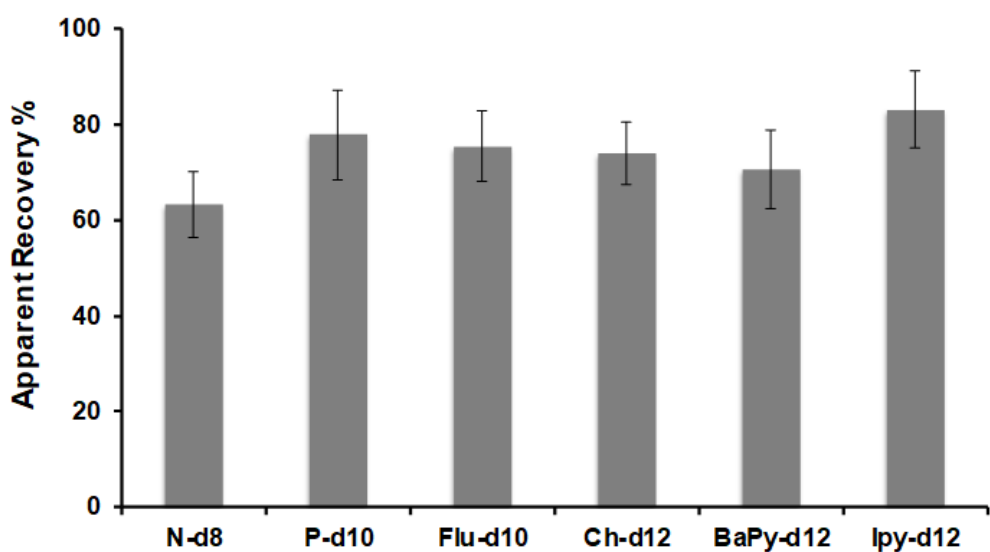


Fig. S4 – Mean percentage values of apparent recovery for the whole analytical procedure of PAH analysis. The meaning of target analyte acronyms is reported in the paragraph S.1.

Table S9 – Method detection (MDL) and quantification (MQL) limits (n=5) for the whole SPE-GC-MS procedure of PAH analysis. Values in bracket represent the standard deviation. The meaning of target analyte acronyms is reported in the paragraph S1.

Compound	MDL (ng L ⁻¹)	MQL (ng L ⁻¹)
N	0.050 (0.001)	0.20 (0.01)
Acy	0.032 (0.001)	0.13 (0.01)
Ac	0.032 (0.001)	0.13 (0.01)
Fl	0.040 (0.001)	0.16 (0.01)
P	0.056 (0.002)	0.22 (0.01)
A	0.056 (0.002)	0.22 (0.01)
Flu	0.042 (0.001)	0.17 (0.01)
Py	0.043 (0.001)	0.17 (0.01)
BaA	0.086 (0.004)	0.34 (0.02)
Ch	0.171 (0.008)	0.68 (0.03)
BbFlu	0.134 (0.007)	0.54 (0.03)
BkFlu	0.134 (0.007)	0.54(0.03)
BaPy	0.179 (0.009)	0.71 (0.04)
BahA	0.226 (0.012)	0.90 (0.05)
Ipy	0.188 (0.010)	0.75 (0.04)
BP	0.226 (0.013)	0.90 (0.05)

S.6 – Kinetic and isotherm tests

The evaluation of biochar and activated carbon adsorption performance towards AP_nEOs and APs was carried out by kinetic and isotherm tests, performed in triplicate. According to the ASTM D-5919-96, suspensions (1 g L⁻¹) of each adsorbent material were prepared and stirred for 24 h. Aliquots of these suspensions were accurately pipetted into amber bottles containing 1 L of target analyte solutions at defined concentrations of AP_nEOs and APs, to achieve a final biochar and MAC concentrations of 10 mg L⁻¹ and 1 mg L⁻¹, respectively. The kinetic and isotherm adsorption tests were performed by maintaining in rotation (Reax 20, Heidolph Instruments, Schwabach, Germany) the bottles under the following experimental conditions: (i) 6 revolutions/minute; (ii) absence of light; (iii) room temperature (25±2°C). The suspensions were finally centrifuged at 30000 x g, for 10 minutes, at 10°C (MPW-351R, MPW Med. Instruments, Warsaw, Poland). A control sample without the sorbent was run in parallel.

Supernatant 1-mL aliquots were stored at +4°C until LC-MS/MS analysis was performed (in any case not later than 24 h after the last collection), according to the following specifications and in accordance with the identification criteria proposed by the Commission Decision 2002/657/CE. The LC-MS/MS analyses were performed on a Shimadzu chromatographic system, consisting of a low pressure gradient quaternary pump Nexera X2 LC-30AD (pump 1) and one isocratic pump LC-20AD XR (pump 2), devoted to the delivery of the post-column positive ionization promoter. A CTO/20AC thermostatic column compartment equipped with the above-mentioned BP analytical column, a SIL-30AC auto injector equipped with a 50 µL sample loop, a DGU-20A 5R degassing unit and a CBM-20A module controller were also used. The entire chromatographic procedure is programmed and automatically controlled by the Analyst® software, version 1.6.2 (Sciex). LC analysis was carried out by injection of 100 µl sample at 50°C, on the BP column, using LC-MS grade water (A) and methanol (B), as eluents, at a flow rate of 0.8 mL min⁻¹ and isocratic elution (85% B) for 4 min. During the whole LC run, the addition of a 300 mM ammonia solution in methanol (i.e. the positive ionization promoter) was post-column dispensed by pump 2 at 40 µL min⁻¹, by means of a three-way connector. Under the aforementioned experimental conditions, total analysis time per sample, including loop filling, was about 4.2 min.

The LC system was coupled with a 5500 QTrap mass spectrometer (Sciex, Ontario, Canada), equipped with a Turbo V® interface by an electro-spray (ESI) probe. MS/MS analysis was carried out using the Multiple Reaction Monitoring (MRM) mode by ESI, both in positive and negative ionization mode. The precursor and product ion pairs, as well as compound-dependent parameters, were optimized by direct infusion of diluted standard solution and are reported in **Table S10**.

Table S10 – LC Retention time (Rt, min) and optimized MS parameters for the detection of quantifier and qualifier ions of ethoxylated alkylphenols and alkylphenols. CE: collision energy (reported in bracket together with the related product ion). DP: declustering potential, EP: entrance potential, CXP: collision cell exit potential. The meaning of target analyte acronyms is reported in the paragraph S1.

Compound	Rt	Precursor ion	Product ions (CE)		DP	EP	CXP	
			Quantifier	Qualifier			Quantifier	Qualifier
4-t-OP ^a	1.16	205	133 (-35)	134 (-25)	-50	-5	-15	-15
4-t-OP ₂ EO ^b	1.60	312	183 (15)	121 (32)	40	5	10	10
4-t-OP ₃ EO ^b	1.79	356	227 (17)	121 (36)	40	5	20	10
4-t-OP ₄ EO ^b	2.00	400	271 (22)	383 (15)	40	5	25	10
4-t-OP ₅ EO ^b	2.19	444	315 (25)	427 (18)	40	5	9	12
4-t-OP ₆ EO ^b	2.39	488	471 (20)	359 (25)	40	5	13	10
4-t-OP ₇ EO ^b	2.60	532	515 (22)	133 (32)	40	5	14	15
4-t-OP ₈ EO ^b	2.83	576	133 (33)	559 (25)	40	5	15	15
4-NP ^a	1.37	219	133 (-45)	147 (-35)	-50	-5	-15	-13
4-NP ₂ EO ^b	1.93	326	183 (15)	121 (33)	45	12	15	13
4-NP ₃ EO ^b	2.19	370	227 (15)	121 (33)	45	12	15	15
4-NP ₄ EO ^b	2.44	414	271 (22)	397 (14)	45	12	30	35
4-NP ₅ EO ^b	2.68	458	315 (23)	441 (17)	45	12	13	13
4-NP ₆ EO ^b	2.93	502	485 (20)	359 (24)	45	12	15	30
4-NP ₇ EO ^b	3.22	546	529 (22)	133 (31)	45	12	17	15
4-NP ₈ EO ^b	3.57	590	133 (33)	573 (23)	45	12	15	13

^a Monitored as $[M-H]^-$ ion; ^b Monitored as $[M + NH_4]^+$ adduct ion.

The first and the second most intense MRM transitions were used for analyte quantification and identification, respectively. Source-dependent parameters were optimized in flow injection analysis at optimal LC flow and mobile phase composition and were as follows: curtain gas 50, CAD gas medium, temperature 650°C, gas 1 40, gas 2 50, interface heater ON and ion spray voltage 3500 V and -4500 V in MRM(+) and MRM(-) mode, respectively. The polarity switching was performed as following specified: (i) from 0 to 1.5 min, MRM(-) for 4-t-OP and 4-NP monitoring and (ii) from 1.5 to 4 min, MRM(+) for 4-t-OP_nEO (with n=2-8) and 4-NP_nEO (with n=2-8) analysis.

Criteria proposed by the Commission Decision 2002/657/CE (The Commission of the European Communities 2002) were adopted for identity confirmation. The positive identification is achieved

when: (i) chromatographic retention time agrees within $\pm 2\%$; (ii) relative abundance of the two transitions, selected as precursor ion and product ion, falls within the permitted tolerances for relative ion intensities using the LC-MS technique. Peak attribution and quantitative determination were performed using MultiQuant software version 3.0.2 (Sciex). All statistical analyses were performed using SPSS® software, version 22 (SPSS Inc., Chicago, IL, USA).

The LC-MS/MS method was preliminary evaluated for instrumental limits of detection (IDLs) and quantification (IQLs), linearity, as well as intra-day and inter-day precision, by replicated injections of standard solutions of APs, Triton™X-45 and IGEPAL® CO-520 technical mixtures in Milli-Q water (**Table S11**). IDLs and IQLs were taken as the minimum concentrations of target analytes that give rise to a S/N equal to 3 and 10, respectively.

The linearity was investigated by replicated analysis ($n=5$) of standard solutions at ten different calibration levels. Concentration ranges from IQLs to 20–500 pg injected were chosen, depending on the response factor of the analyte considered, in order to cover a linearity range of about two magnitude orders. Determination coefficients (R^2) ≥ 0.9906 were obtained in all cases.

Intra-day ($RSD\%_{intra}$) and inter-day ($RSD\%_{inter}$) precision were evaluated by ten replicated injections of standard solutions, at concentration levels twice higher than IQLs. $RSD\%_{intra}$ and $RSD\%_{inter}$ values were found in the ranges of 1.8-4.6% and 2.4-5.6%, respectively.

The matrix effect was evaluated through the matrix matched calibration method, by spiking the matrix and Milli-Q water with the following concentration of APs, Triton™X-45 (4-t-OPnEO) and IGEPAL® CO-520 (4-NPnEO) technical mixtures. AP_nEOs technical mixtures: 0, 5, 10, 25, 50, 75, 100, 150, 200, 300 and 400 $\mu\text{g L}^{-1}$; APs: 0, 0.5, 1.0, 2.5, 5.0, 7.5, 10, 15, 20, 30 and 40 $\mu\text{g L}^{-1}$.

Table S11 – Instrumental limits (pg injected) of detection (IDLs), and quantification (IQLs)^a, linearity range, determination coefficients (R^2), intra-day ($RSD\%_{intra}$) and inter-day ($RSD\%_{inter}$) relative standard deviation percentages (n=5) of the LC-MS/MS method. The meaning of target analyte acronyms is reported in the paragraph S1.

Compound	IDL	Linearity range ^a	R^2	$RSD\%_{intra}$	$RSD\%_{inter}$
4-t-OP	2.90	9.50-500	0.9952	2.4	3.6
4-t-OP ₂ EO	0.10	0.35-75	0.9951	2.0	2.7
4-t-OP ₃ EO	0.05	0.20-110	0.9910	2.1	2.6
4-t-OP ₄ EO	0.04	0.15-110	0.9939	1.8	2.4
4-t-OP ₅ EO	0.07	0.25-80	0.9906	2.2	2.9
4-t-OP ₆ EO	0.14	0.45-50	0.9937	3.2	4.3
4-t-OP ₇ EO	0.16	0.55-35	0.9936	4.1	4.8
4-t-OP ₈ EO	0.13	0.45-20	0.9918	4.6	5.3
4-NP	1.70	5.50-500	0.9921	2.5	3.6
4-NP ₂ EO	0.63	2.10-75	0.9955	2.5	3.1
4-NP ₃ EO	0.32	1.05-90	0.9971	2.2	2.9
4-NP ₄ EO	0.18	0.60-90	0.9933	2.9	4.0
4-NP ₅ EO	0.26	0.90-75	0.9987	2.3	2.9
4-NP ₆ EO	0.45	1.50-55	0.9939	3.0	3.8
4-NP ₇ EO	0.66	2.20-40	0.9922	4.1	5.0
4-NP ₈ EO	0.45	1.50-30	0.9973	4.3	5.6

^a The bottom limits of linearity range represent IQLs.

Direct injections (n = 3) of 50 μ L of spiked purified matrix aliquots and Milli-Q reference solutions were performed, and the mean peak areas obtained were plotted as a function of the spiked concentrations. Matrix effect percentage (ME%) was defined as:

$$ME\% = \left(\frac{S_{matrix}}{S_{solvent}} * 100 \right) - 100$$

where S_{matrix} and $S_{solvent}$ are the slopes of the calibration lines in matrix and in Milli-Q water, respectively. ME% values higher or lower than zero indicate the presence of signal enhancement or suppression in comparison with the instrumental response observed in Milli-Q water (see **Table S12**). However, absolute values of $ME\% \leq 20\%$ are commonly considered not significant. Data herein obtained for MAC evidenced a suppressive ME% values ranging from -4.0% to -11.4% , whereas for BC450-850, a signal enhancement, included between 0.8% and 19.1% was observed.

Table S12 – Mean values (n=3) and standard deviations (in brackets) of matrix effect in biochars and activated carbon. The meaning of target analyte acronyms is reported in the paragraph S1.

Compound	Matrix Effect (%)			
	MAC	BC450	BC650	BC850
4-t-OP	-8.2 (0.7)	5.2 (3.7)	0.8 (2.3)	6.7 (3.4)
4-t-OP ₂ EO	-7.7 (0.5)	13.6 (1.9)	3.9 (1.4)	10.0 (1.3)
4-t-OP ₃ EO	-5.0 (0.2)	12.6 (2.5)	2.3 (1.6)	10.8 (1.5)
4-t-OP ₄ EO	-6.8 (0.4)	10.5 (2.9)	2.1 (0.7)	12.4 (1.0)
4-t-OP ₅ EO	-4.0 (0.5)	16.4 (2.4)	6.2 (1.2)	12.3 (1.8)
4-t-OP ₆ EO	-4.6 (0.5)	18.3 (3.7)	6.2 (1.1)	14.6 (2.0)
4-t-OP ₇ EO	-5.7 (0.4)	16.5 (3.3)	5.4 (1.0)	14.2 (2.4)
4-t-OP ₈ EO	-7.4 (0.3)	17.7 (4.2)	3.9 (2.3)	6.8 (1.9)
4-NP	-7.8 (0.6)	10.8 (4.2)	2.3 (1.7)	13.5 (3.9)
4-NP ₂ EO	-7.1 (0.3)	19.1 (3.5)	3.2 (1.1)	13.5 (1.5)
4-NP ₃ EO	-5.1 (0.5)	9.3 (2.7)	2.7 (1.3)	13.5 (1.7)
4-NP ₄ EO	-8.1 (0.6)	6.7 (4.5)	2.8 (1.4)	11.2 (1.2)
4-NP ₅ EO	-7.7 (0.2)	13.8 (4.8)	3.3 (1.9)	10.2 (0.8)
4-NP ₆ EO	-11.4 (1.0)	11.4 (5.3)	3.9 (1.8)	8.3 (1.1)
4-NP ₇ EO	-8.5 (0.7)	17.9 (6.2)	8.7 (4.5)	9.6 (3.9)
4-NP ₈ EO	-5.7 (1.2)	15.1 (6.3)	6.1 (5.0)	10.5 (5.7)

S.6.1 Kinetic adsorption tests

Complete removal datasets for APs and AP_nEOs are shown in **Tables S13-S16** for BC450, BC650, BC850 and MAC, respectively.

Table S13 – Mean values (n=3) and standard deviation (in brackets) of removal percentages of AP_nEOs and APs from wastewater solutions (4-t-OP and 4-NP = 100 µg L⁻¹; technical mixtures containing AP_nEOs = 1 mg L⁻¹) by 10 mg L⁻¹ of BC450 at different contact times. Within a same compound, values with the same letter are not statistically different ($P>0.05$) according to the Dunnett T3 non-parametric test. The meaning of target analyte acronyms is reported in the paragraph S1.

Compound	Removal percentages				
	1h	2h	4h	6h	12h
4-t-OP	19 (2) a	30 (1) b	32 (2) b	30 (4) b	32 (2) b
4-t-OP ₂ EO	30 (6) a	45 (1) b	47 (2) b	47 (1) b	48 (2) b
4-t-OP ₃ EO	37 (3) a	53 (2) b	55 (3) b	53 (4) b	55 (1) b
4-t-OP ₄ EO	37 (2) a	51 (2) b	49 (5) b	51 (5) b	52 (2) b
4-t-OP ₅ EO	38 (3) a	52 (2) b	52 (2) b	52 (6) b	53 (4) b
4-t-OP ₆ EO	38 (2) a	53 (3) b	53 (3) b	53 (2) b	55 (1) b
4-t-OP ₇ EO	39 (2) a	52 (3) b	51 (3) b	53 (2) b	51 (1) b
4-t-OP ₈ EO	25 (2) a	43 (3) b	44 (3) b	46 (3) b	42 (3) b
4-NP	38 (2) a	54 (2) b	54 (2) b	51 (3) b	54 (3) b
4-NP ₂ EO	61 (3) a	79 (1) b	78 (2) b	79 (1) b	79 (2) b
4-NP ₃ EO	69 (4) a	81 (1) b	79 (3) b	82 (1) b	80 (4) b
4-NP ₄ EO	65 (2) a	80 (2) b	80 (3) b	82 (3) b	80 (3) b
4-NP ₅ EO	66 (2) a	82 (2) b	81 (1) b	81 (1) b	79 (2) b
4-NP ₆ EO	59 (2) a	71 (4) b	71 (4) b	72 (4) b	70 (2) b
4-NP ₇ EO	51 (2) a	64 (1) b	63 (2) b	64 (2) b	64 (3) b
4-NP ₈ EO	49 (4) a	61 (1) b	62 (2) b	61 (2) b	61 (4) b

Table S14 – Mean values (n=3) and standard deviation (in brackets) of removal percentages of APnEOs and APs from wastewater solutions (4-t-OP and 4-NP = 100 µg L⁻¹; technical mixtures containing APnEOs = 1 mg L⁻¹) by 10 mg L⁻¹ of BC650 at different contact times. Within a same compound, values with the same letter are not statistically different ($P>0.05$) according to the Dunnett T3 non-parametric test. The meaning of target analyte acronyms is reported in the paragraph S1.

Compound	Removal percentages				
	1h	2h	4h	6h	12h
4-t-OP	27 (2) a	39 (1) b	41 (5) b	39 (5) b	41 (4) b
4-t-OP ₂ EO	42 (6) a	62 (3) b	60 (2) b	62 (2) b	60 (1) b
4-t-OP ₃ EO	37 (1) a	56 (3) b	62 (7) b	63 (6) b	62 (4) b
4-t-OP ₄ EO	42 (4) a	65 (2) b	65 (4) bc	62 (5) c	66 (4) bc
4-t-OP ₅ EO	35 (2) a	59 (1) b	59 (3) b	60 (6) b	61 (3) b
4-t-OP ₆ EO	43 (1) a	57 (1) b	59 (2) bc	54 (1) b	57 (3) bc
4-t-OP ₇ EO	27 (3) a	38 (1) b	39 (3) b	39 (2) b	42 (3) b
4-t-OP ₈ EO	29 (3) a	40 (1) b	42 (2) c	42 (1) c	40 (2) bc
4-NP	51 (2) a	78 (1) b	76 (2) bc	75 (2) c	79 (4) bc
4-NP ₂ EO	61 (6) a	82 (2) b	80 (2) b	84 (2) b	80 (2) b
4-NP ₃ EO	50 (3) a	83 (1) b	82 (1) b	84 (1) b	83 (1) b
4-NP ₄ EO	64 (1) a	80 (1) b	80 (2) b	83 (1) b	83 (2) b
4-NP ₅ EO	64 (4) a	78 (2) b	80 (1) b	80 (2) b	80 (2) b
4-NP ₆ EO	53 (1) a	64 (5) b	64 (2) b	67 (4) b	67 (1) b
4-NP ₇ EO	40 (2) a	65 (1) b	66 (1) b	66 (3) b	67 (3) b
4-NP ₈ EO	48(3) a	63 (2) b	61 (3) b	62 (3) b	658 (1) b

Table S15 – Mean values (n=3) and standard deviation (in brackets) of removal percentages of APnEOs and APs from wastewater solutions (4-t-OP and 4-NP = 100 µg L⁻¹; technical mixtures containing APnEOs = 1 mg L⁻¹) by 10 mg L⁻¹ of BC850 at different contact times. Within a same compound, values with the same letter are not statistically different ($P>0.05$) according to the Dunnett T3 non-parametric test. The meaning of target analyte acronyms is reported in the paragraph S1.

Compound	Removal percentages				
	1h	2h	4h	6h	12h
4-t-OP	22 (2) a	40 (2) b	43 (2) b	43 (2) b	437 (2) b
4-t-OP ₂ EO	44 (2) a	63 (2) b	62 (4) b	66 (2) b	65 (2) b
4-t-OP ₃ EO	44 (3) a	64 (5) b	67 (4) b	68 (2) b	70 (2) b
4-t-OP ₄ EO	46 (3) a	68 (3) b	66 (1) b	69 (3) b	68 (3) b
4-t-OP ₅ EO	46 (3) a	65 (1) b	67 (1) c	66 (4) bc	65 (2) bc
4-t-OP ₆ EO	43 (2) a	63 (1) b	66 (4) bc	66 (2) c	64 (4) bc
4-t-OP ₇ EO	39 (2) a	56 (1) b	55 (1) b	56 (2) b	56 (1) b
4-t-OP ₈ EO	36 (2) a	47 (3) b	49 (4) b	52 (6) b	51 (3) b
4-NP	52 (2) a	67 (1) b	69 (1) bc	70 (1) c	71 (1) c
4-NP ₂ EO	56 (4) a	81 (1) b	81 (1) b	79 (3) b	80 (2) b
4-NP ₃ EO	67 (1) a	82 (1) b	84 (1) bc	86 (1) c	86 (1) c
4-NP ₄ EO	68 (1) a	84 (1) b	85 (1) b	85 (1) b	86 (2) b
4-NP ₅ EO	52 (2) a	76 (1) b	74 (3) b	77 (2) b	80 (3) b
4-NP ₆ EO	50 (4) a	71 (1) b	72 (2) b	72 (2) b	74 (2) b
4-NP ₇ EO	42 (2) a	66 (2) b	67 (2) b	68 (2) b	68 (3) b
4-NP ₈ EO	37 (3) a	59 (1) b	61 (3) bc	63 (2) c	62 (2) bc

Table S16 – Mean values (n=3) and standard deviation (in brackets) of removal percentages of APnEOs and APs from wastewater solutions (4-t-OP and 4-NP = 100 $\mu\text{g L}^{-1}$; technical mixtures containing APnEOs = 1 mg L^{-1}) by 1 mg L^{-1} of MAC at different contact times. Within a same compound, values with the same letter are not statistically different ($P>0.05$) according to the Dunnett T3 non-parametric test. The meaning of target analyte acronyms is reported in the paragraph S1.

Compound	Removal percentages				
	1h	2h	4h	6h	12h
4-t-OP	42 (1) a	58 (4) b	58 (2) b	57 (7) b	61 (5) b
4-t-OP2EO	57 (4) a	76 (1) b	78 (4) b	76 (3) b	78 (1) b
4-t-OP3EO	62 (2) a	80 (1) b	81 (1) b	80 (2) b	81 (1) b
4-t-OP4EO	62 (3) a	78 (1) b	78 (2) b	78 (1) b	79 (1) b
4-t-OP5EO	57 (5) a	73 (1) b	76 (3) bc	76 (2) c	75 (2) bc
4-t-OP6EO	52 (3) a	73 (3) b	71 (2) b	72 (1) b	72 (6) b
4-t-OP7EO	48 (5) a	69 (3) b	69 (2) b	68 (1) b	67 (5) b
4-t-OP8EO	49 (4) a	64 (4) b	65 (2) b	64 (2) b	64 (3) b
4-NP	52 (6) a	89 (1) b	92 (1) b	87 (4) b	91 (7) b
4-NP2EO	65 (1) a	87 (1) b	88 (2) b	89 (3) b	87 (3) b
4-NP3EO	71 (3) a	91 (1) b	90 (5) b	91 (1) b	939 (1) b
4-NP4EO	63 (4) a	90(1) b	90 (1) b	90 (1) b	92 (1) b
4-NP5EO	53 (3) a	87 (1) b	87 (1) b	87 (3) b	88 (4) b
4-NP6EO	63 (4) a	84 (1) b	84 (2) b	83 (4) b	84 (2) b
4-NP7EO	51 (4) a	78 (4) b	80 (1) b	79 (4) b	80 (4) b
4-NP8EO	52 (1) a	73 (1) b	72 (1) b	73 (2) b	71 (1) b

S.6.2 Isotherm adsorption tests

Complete datasets regarding Langmuir maximum sorption parameters (Q_m) and binding energy constants (k) are shown in **Table S17** and **Table S18**, respectively.

Table S17 – Mean values (n=3) standard deviation (in brackets) of maximum sorption parameters (Q_m) as estimated by Langmuir adsorption-isotherm linear equation in the ranges 5–100 $\mu\text{g L}^{-1}$ ($Q_{m,1}$ - Range 1) and 100–400 $\mu\text{g L}^{-1}$ ($Q_{m,2}$ - Range 2) of APEOs technical mixtures and APs for 10 mg L^{-1} and 1 mg L^{-1} of biochars and mineral activated carbon, respectively. The meaning of target analyte acronyms is reported in the paragraph S1.

Analyte	Adsorption Maxima (Q_m) mg g^{-1}							
	$Q_{m,1}$ - Range 1				$Q_{m,2}$ - Range 2			
	BC450	BC650	BC850	MAC	BC450	BC650	BC850	MAC
4-t-OP	3.8 (0.1)	6.2 (0.2)	5.3 (0.1)	103 (10)	11 (1)	17.2 (0.9)	24 (3)	386 (9)
4-t-OP ₂ EO	0.89 (0.06)	1.29 (0.08)	1.43 (0.02)	16.6 (0.6)	3.4 (0.3)	5.2 (0.3)	5.5 (0.3)	47 (1)
4-t-OP ₃ EO	1.56 (0.04)	2.0 (0.1)	2.0 (0.1)	24 (2)	6.6 (0.5)	7.2 (0.3)	7.86 (0.09)	60.7 (0.2)
4-t-OP ₄ EO	1.53 (0.05)	2.2 (0.1)	1.94 (0.05)	24 (2)	6.3 (0.1)	7.7 (0.5)	7.8 (0.2)	53 (2)
4-t-OP ₅ EO	1.18 (0.07)	1.64 (0.02)	1.5 (0.1)	17.1 (0.8)	4.9 (0.1)	5.6 (0.3)	5.3 (0.2)	39 (1)
4-t-OP ₆ EO	0.74 (0.05)	0.92 (0.05)	1.0 (0.1)	11.1 (0.4)	2.74 (0.08)	2.8 (0.1)	3.7 (0.5)	25.5 (0.6)
4-t-OP ₇ EO	0.42 (0.01)	0.40 (0.01)	0.37 (0.05)	6.8 (0.1)	1.82 (0.06)	1.1 (0.1)	1.3 (0.2)	16.6 (0.1)
4-t-OP ₈ EO	0.20 (0.01)	0.25 (0.01)	0.25 (0.02)	3.7 (0.1)	0.83 (0.09)	0.72 (0.03)	0.95 (0.06)	7.5 (0.4)
4-NP	6.8 (0.2)	8.8 (0.4)	9.6 (0.6)	164 (13)	20.7 (0.7)	31 (2)	42 (2)	625 (27)
4-NP ₂ EO	1.47 (0.09)	1.75 (0.09)	1.83 (0.03)	17.8 (0.5)	5.5 (0.1)	7.6 (0.7)	7.6 (0.2)	73 (2)
4-NP ₃ EO	1.9 (0.1)	2.2 (0.1)	2.0 (0.1)	23 (2)	6.5 (0.2)	10 (0.4)	8.1 (0.7)	78 (2)
4-NP ₄ EO	1.96 (0.07)	1.90 (0.04)	2.0 (0.2)	20.3 (0.7)	6.8 (0.2)	9.0 (0.2)	8.7 (0.9)	68.6 (0.5)
4-NP ₅ EO	1.37 (0.02)	1.40 (0.08)	1.40 (0.06)	15.5 (0.2)	5.1 (0.2)	6.3 (0.2)	6.9 (0.5)	54.8 (0.1)
4-NP ₆ EO	0.97 (0.04)	1.00 (0.08)	1.0 (0.1)	11.8 (0.1)	3.9 (0.2)	4.1 (0.3)	4.2 (0.3)	41.3 (0.2)
4-NP ₇ EO	0.56 (0.02)	0.58 (0.05)	0.55 (0.04)	8.4 (0.2)	2.9 (0.1)	2.2 (0.1)	2.36 (0.08)	34.5 (0.1)
4-NP ₈ EO	0.41 (0.01)	0.41 (0.01)	0.41 (0.01)	5.6 (0.1)	1.3 (0.1)	1.40 (0.06)	1.67 (0.09)	20.2 (0.3)

Table S18 – Mean values (n=3) standard deviation (in brackets) of binding energy constants (k) as estimated by Langmuir adsorption-isotherm linear equation in the ranges 5–100 $\mu\text{g L}^{-1}$ (k_1 - Range 1) and 100–400 $\mu\text{g L}^{-1}$ (k_2 - Range 2) of APEOs technical mixtures and APs for 10 mg L^{-1} and 1 mg L^{-1} of biochars and mineral activated carbon, respectively. The meaning of target analyte acronyms is reported in the paragraph S1.

Analyte	Binding energy constants (k)							
	k_1 - Range 1				k_2 - Range 2			
	BC450	BC650	BC850	MAC	BC450	BC650	BC850	MAC
4-t-OP	0.132 (0.01)	0.188 (0.02)	0.106 (0.01)	0.094 (0.02)	0,008 (0.01)	0.0104 (0.00)	0.004 (0.00)	0.008 (0.00)
4-t-OP ₂ EO	7.437 (3.45)	0.856 (0.07)	0.997 (0.06)	1.602 (0.18)	0,029 (0.01)	0.0594 (0.01)	0.075 (0.01)	0.157 (0.00)
4-t-OP ₃ EO	0.684 (0.17)	0.507 (0.04)	0.902 (0.16)	1.217 (0.25)	0,029 (0.01)	0.0413 (0.01)	0.045 (0.00)	0.119 (0.01)
4-t-OP ₄ EO	0.776 (0.16)	0.296 (0.03)	0.865 (0.02)	1.301 (0.26)	0,043 (0.01)	0.0391 (0.01)	0.044 (0.00)	0.165 (0.01)
4-t-OP ₅ EO	0.962 (0.31)	0.661 (0.02)	1.192 (0.26)	1.947 (0.32)	0,069 (0.00)	0.0649 (0.01)	0.072 (0.01)	0.247 (0.01)
4-t-OP ₆ EO	1.752 (0.40)	1.398 (0.17)	1.419 (0.24)	3.413 (0.31)	0,080 (0.00)	0.1100 (0.01)	0.085 (0.02)	0.363 (0.03)
4-t-OP ₇ EO	1.456 (0.06)	2.004 (0.21)	2.569 (1.19)	6.096 (0.91)	0,156 (0.02)	0.1338 (0.03)	0.097 (0.03)	0.561 (0.04)
4-t-OP ₈ EO	5.361 (0.77)	6.254 (0.10)	0.127 (0.02)	12.31 (0.25)	0,009 (0.00)	0.3242 (0.01)	0.009 (0.00)	1.754 (0.01)
4-NP	0.374 (0.12)	0.415 (0.03)	5.960 (0.58)	0.235 (0.02)	0,107 (0.00)	0.0265 (0.02)	0.194 (0.03)	0.023 (0.00)
4-NP ₂ EO	2.127 (0.33)	2.218 (0.42)	1.763 (0.12)	7.007 (0.39)	0,120 (0.01)	0.1688 (0.03)	0.133 (0.01)	0.415 (0.03)
4-NP ₃ EO	1.753 (0.18)	1.289 (0.05)	0.946 (0.13)	4.786 (0.70)	0,125 (0.00)	0.0937 (0.00)	0.067 (0.01)	0.340 (0.03)
4-NP ₄ EO	1.522 (0.20)	1.899 (0.11)	0.830 (0.15)	5.340 (0.61)	0,119 (0.02)	0.0986 (0.00)	0.051 (0.01)	0.363 (0.01)
4-NP ₅ EO	2.449 (0.38)	2.363 (0.29)	2.041 (0.20)	7.474 (0.30)	0,095 (0.01)	0.0956 (0.01)	0.088 (0.01)	0.363 (0.01)
4-NP ₆ EO	1.825 (0.32)	2.618 (0.46)	2.455 (0.42)	8.013 (0.10)	0,084 (0.01)	0.1052 (0.01)	0.092 (0.02)	0.412 (0.01)
4-NP ₇ EO	5.693 (0.77)	4.233 (0.74)	4.185 (0.77)	9.273 (0.09)	0,244 (0.06)	0.1089 (0.01)	0.083 (0.00)	0.397 (0.01)
4-NP ₈ EO	4.900 (0.60)	7.725 (0.31)	7.094 (0.88)	15.97 (0.84)	0,008 (0.06)	0.2394 (0.01)	0.169 (0.01)	0.725 (0.01)

The complete dataset regarding the Freundlich adsorption parameters (n) is shown in **Table S19**.

Table S19 – Mean ($n=3$) and standard deviations (in brackets) of Freundlich adsorption intensity (n) parameters, calculated for biochars (BC) produced at 450, 650, 850°C, and mineral activated carbon (MAC), in the ranges 5–400 $\mu\text{g L}^{-1}$ for AP_{*n*}EO technical mixtures, and in the ranges 0.5–40 $\mu\text{g L}^{-1}$ for APs. See Table 1 for the meaning of target analyte acronyms.

Compound	n			
	BC450	BC650	BC850	MAC
4-t-OP	2.12 (0.033)	2.15 (0.046)	1.86 (0.021)	1.57 (0.040)
4-t-OP ₂ EO	2.07 (0.052)	1.62 (0.038)	1.61 (0.031)	1.75 (0.034)
4-t-OP ₃ EO	1.83 (0.062)	1.65 (0.020)	1.82 (0.037)	1.86 (0.036)
4-t-OP ₄ EO	1.87 (0.092)	1.47 (0.013)	1.75 (0.008)	1.91 (0.049)
4-t-OP ₅ EO	1.80 (0.097)	1.61 (0.007)	1.78 (0.096)	1.92 (0.054)
4-t-OP ₆ EO	1.92 (0.064)	1.83 (0.035)	1.70 (0.024)	1.96 (0.026)
4-t-OP ₇ EO	1.71 (0.014)	2.00 (0.030)	2.06 (0.260)	1.97 (0.044)
4-t-OP ₈ EO	2.10 (0.027)	2.12 (0.045)	2.06 (0.033)	2.05 (0.026)
4-NP	2.35 (0.137)	1.83 (0.014)	1.55 (0.043)	1.45 (0.009)
4-NP ₂ EO	1.78 (0.061)	1.54 (0.066)	1.53 (0.027)	1.68 (0.007)
4-NP ₃ EO	1.79 (0.063)	1.55 (0.020)	1.56 (0.019)	1.75 (0.045)
4-NP ₄ EO	1.70 (0.048)	1.64 (0.030)	1.56 (0.020)	1.80 (0.021)
4-NP ₅ EO	1.86 (0.037)	1.83 (0.048)	1.75 (0.024)	1.91 (0.010)
4-NP ₆ EO	1.75 (0.054)	1.83 (0.020)	1.82 (0.032)	1.88 (0.011)
4-NP ₇ EO	2.12 (0.041)	2.05 (0.022)	2.04 (0.035)	1.80 (0.023)
4-NP ₈ EO	1.95 (0.025)	2.10 (0.023)	2.05 (0.056)	1.90 (0.057)